UNIVERSITY OF CALIFORNIA, SAN DIEGO

Characterization of a Coral Rhesus Protein, a Putative NH_3 Gas Channel

A Thesis submitted in partial satisfaction of the

Requirements for the degree

Master of Science

in

Marine Biology

by

Angus Blacklaw Thies

Committee in charge:

Professor Martin Tresguerres, Chair
Professor Amro Hamdoun
Professor Greg Rouse

2018

The Thesis of Angus Blacklaw Thies is approved, and it is acceptable in quality and form for publication on microfilm and electronically:

Chair

University of California, San Diego

2018

DEDICATION

I'd like to dedicate this thesis to all those who made its creation possible including my family, friends, and colleagues. Additionally, I would like to single out several individuals who deserve special recognition for their contributions in aiding me in my struggle. First, Carrie and Rocky Thies, my parents, who provided sage council, weathered ears, and endless support for the past year. Not only have they done everything in their power to help me succeed, they have continuously pushed me to pursue my interests and challenge myself. Their care and support has not gone unnoticed and I am eternally grateful to be blessed with their love.

Second, Austin Thies, my brother, who has always been a source of laughter and friendship in my life. Time and time again you have shown me that hard work pays off and that struggle is the forge whereby character is fashioned.

Third, all the members of the Tresguerres Lab who have offered their guidance, advice, humor, and support during the past year. I could not have asked for a better group of friends to work alongside. My advisor, Dr. Martin Tresguerres, deserves to be singled out as he has been a positive force in my life who has challenged me to think critically about my own work, accept criticism, and strive to produce honest science worthy of publication. His *patience*, drive, and humor will not be forgotten. In addition, Dr. Megan Liu has my deepest thanks for taking me under her wing and mentoring me during my time in the Tresguerres lab. Her friendship and *patience* made this work possible and I thank her for it.

Finally, Dr. Greg Rouse and Dr. Amro Hamdoun, thank you for serving on my thesis committee, providing support for my work, and aiding me in the completion of my research.

EPIGRAPH

"I am among those who think that science has great beauty."
-Marie Curie

"Science is not only a disciple of reason but, also, one of romance and passion."
-Stephen Hawking

"Nothing in this world can take the place of persistence.
Talent will not: nothing is more common than unsuccessful men with talent.
Genius will not; unrewarded genius is almost a proverb.
Education will not: the world is full of educated derelicts.
Persistence and determination alone are omnipotent. The slogan "Press On" has solved and will always solve the problems of the human race."
-Calvin Coolidge

"In questions of science, the authority of a thousand is not worth the humble reasoning of a single individual."
-Galileo Galilei

"That's not what your mother said…"
-Martin Tresguerres

TABLE OF CONTENTS

LIST OF ABBREVIATIONS

Amt	Ammonium transport protein
ATP	Adenosine triphosphate
ayRh	*Acropora yongei* Rhesus Protein
CA	Carbonic anhydrase
$CaCO_3$	Calcium carbonate
CCM	Carbon concentrating mechanism
DIC	Dissolved inorganic carbon; CO_2, HCO_3^-, and CO_3^{2-}
GFP	Green fluorescent protein
H^+	Proton/hydrogen ion/acid molecule
HCN	Hyperpolarization-activated cyclic nucleotide-gated potassium channel
Mep	Methylammonium permeases
NCM	Nitrogen concentrating mechanism
NH_3	Ammonia gas
NH_4^+	Ammonium ion
NHE	Sodium-Hydrogen Exchanger (Na^+-H^+ Exchanger)
NKA	Sodium-Potassium ATPase (Na^+-K^+-ATPase)
PBS	Phosphate buffered saline
PBS-TX	Phosphate buffered saline, 0.2% Triton-X
pH_c	Cytoplasmic pH
Rh	Rhesus protein
SCM	Subcalicoblastic medium
Slc4	Bicarbonate transporters (HCO_3^- transporters)
SOM	Skeletal organic matrix
VHA	Vacuolar-type Proton-ATPase (H^+-ATPase)

LIST OF FIGURES

LIST OF TABLES

ACKNOWLEDGEMENTS

This work contains material that is being prepared for publication: Thies A, Barron M, Tresguerres M. An Rh protein in coral constitutes a novel diel nitrogen concentrating mechanism to regulate *Symbiodinium* growth. *American Journal of Physiology – Cell Physiology*.

ABSTRACT OF THE THESIS

Characterization of a Coral Rhesus Protein, a Putative NH_3 Gas Channel

by

Angus Blacklaw Thies

Master of Science in Marine Biology

University of California, San Diego, 2018

Professor Martin Tresguerres, Chair

Coral reefs ecosystems are facing mounting threats in the Anthropocene Era, yet basic coral biology remains largely uncharacterized. An essential and unexplored physiological mechanism in corals is the transport of nitrogenous molecules such as NH_3/NH_4^+. The goal of this thesis is to characterize the molecular and cellular mechanisms of *Acropora yongei* which enable nitrogen excretion and metabolic exchange between the coral animal and symbiotic *Symbiodinium*. This is the first study to utilize molecular and immunohistochemistry techniques to investigate the role of a Cnidarian Rh protein, a putative NH_3 gas channel. Phylogenetic analysis determined *A. yongei* Rh (ayRh) is part of the Rhp1 protein subgroup, members of which are capable

of transporting NH_3 and possibly CO_2 gasses along partial pressure gradients. ayRh was colocalized with the vacuolar H^+-ATPase (VHA) on the symbiosome membrane constituting a novel nitrogen concentrating mechanism (NCM). ayRh-dependent NH_3/NH_4^+ supply to *Symbiodinium* appears to vary on a diel cycle, possibly as a mechanism that allows coral host cells to regulate symbiont metabolism and growth. Preliminary evidence also suggests VHA may traffic with ayRh in a protein complex. Continuously high levels of ayRh are also observable in desmocytes, cells that facilitate skeletal attachment. Here, diffusion of NH_3 via ayRh may play a role in regulating the pH of the calcifying environment or in integration with the aboral mesoglea. Finally, ayRh was localized to the oral ectoderm where it appears to facilitate nitrogenous waste excretion into seawater, possibly enhanced by microvilli movement akin to ciliary beating in mussels.

INTRODUCTION

Coral reef economies, health, and status

Coral reef ecosystems are hotspots of biodiversity that are home to diverse assemblages of fish, invertebrate, and microbial species (Sala & Knowlton 2006), and are of particular interest to humans. Reefs cover only 0.1-0.5% of the ocean floor (Cooper 1994, Spalding & Grenfell 1997) yet they supply 10% of all human-consumed fish (Smith 1978). More than 100 countries have coastline bordered by coral reefs where recreation and tourism also contribute to national economies. The physical structure of the reef provides economic value by protecting coastal regions from storm damage and slowing erosion (Knowlton et al. 2010). The scientific value of reef-specific organisms can also not be understated as many are of particular interest to pharmaceutical companies. A myriad of biologically active compounds has been isolated from reef sponges, cnidarians, seaweeds, and symbiotic microorganisms exhibiting anticancer, antimicrobial, anti-inflammatory, and AIDS-inhibiting properties (Carté 1996). Given their importance, it is alarming that global coral reef-health is rapidly declining in response to anthropogenic stressors. Rising sea surface temperatures, ocean acidification, pollution, and overfishing are increasing reef susceptibility to existing physical and biological stressors such as hurricanes, eutrophication, diseases, and invasive species, resulting in coral mass mortality events (Hughes & Connell 1999, Davy et al. 2012). Some current models predict that up to a third of all coral species will become extinct by the end of the 21st century (Carpenter et al. 2008) and conclude that preserving existing biological configurations of reefs is no

longer possible; anthropogenic intervention to maintain reefs' biological functions will instead be required in the Anthropocene Era (Hughes et al. 2017).

Many studies have been conducted to assess coral reef susceptibility to anthropogenic stressors. A substantial portion of these studies focus on assessing overall reef-health through observational methods and species quantification (*Acropora spp., Diadema antillarum*) (Lirman et al. 2010, Aronson et al. 2002) using on-site man-power (Carpenter et al. 2008). While those types of studies are certainly important for assessing current reef-health and generating support for conservation plans, they do little to explain the physiological mechanisms behind the observed coral declines. This gap in mechanistic knowledge has been identified by a number of authors (Downs et al. 2005, Weis & Allemand 2009, Weis et al. 2008) and focus has begun to include bottom-up studies on the physiological mechanisms of corals in addition to top-down observational studies of whole-reef systems.

A number of recent studies have made significant advancements in understanding coral cell biology, a field that has historically received little to no attention. As a result, we are just beginning to understand the basic mechanisms behind essential life processes including calcification, coral bleaching, and the coral-*Symbiodinium* relationship. One such study discovered that coral host cells promote photosynthesis by their symbiotic algae through concentrating CO_2 using vacuolar H^+-ATPases (VHA) (Barott et al. 2015a); this mechanism was present in both *A. yongei* and *S. pistillata*. Understanding basic mechanisms such as this are prerequisites to understanding and predicting coral responses to stress. However, not all corals utilize the same cellular mechanisms to accomplish the same processes. Another study

detected differences in the cellular localization of key ion-transporting proteins between *A. yongei* and *Stylophora pistillata* (Barott et al. 2015b). Because these proteins are involved in HCO_3^- and Ca^{2+} delivery to calicoblastic cells and symbiotic algae, that study suggested species-specific mechanisms for calcification and photosynthesis. These differences potentially provide mechanistic bases for differential susceptibility, resilience, and adaptability to environmental change. A union of ecological studies and characterization of common and species-specific physiological coral mechanisms is therefore essential to drafting comprehensive management strategies to preserve the biological integrity of coral systems in the Anthropocene era.

General coral taxonomy, anatomy, and terminology

Corals are colonial animals of the phylum Cnidaria, closely related to jellyfish and anemones. Reef-building corals (Scleractinia) can be divided into two distinct clades, Robust and Complex, which diverged between 300-400Mya (Romano & Cairns 2000, Romano & Palumbi 1996, Stolarski et al. 2011). Their common ancestor did not calcify, suggesting that both clades evolved calcification mechanisms independently and may present clade- or species-specific mechanisms (Tresguerres et al. 2017). Supporting this idea, corals in the Robust clade (e.g. *Stylophora, Pocillopora, Orbicella*) have more heavily-calcified skeletons compared to those in the Complex clade (e.g. *Acropora, Porites, Siderastrea*), which additionally present greater skeleton-tissue interweaving. This evolutionary pattern likely applies to other physiological mechanisms that may determine clade or species-specific responses to environmental stress.

All cnidarians are diploblastic with two distinct germ layers: an ectoderm and an endoderm (the term ‘gastroderm’ has been used interchangeably with ‘endoderm’ in

literature). These layers are separated by a vascular cavity: the coelenteron. The coelenteron is flanked on either side by both an ecto- and endodermal cell layer resulting in a colony four-layers-thick (Fig. 1). Below the living animal is a calcium carbonate ($CaCO_3$) skeleton which the colony builds over its lifetime (Fig. 1). Tissue layers proximal to seawater are the oral ectoderm and oral endoderm and those proximal to the skeleton are the aboral endoderm and aboral ectoderm. Oral and aboral tissue pairs are joined by mesoglea, an extracellular matrix comprised of connective protein fibers (Phillips 1963). While typical corals possess all four tissue layers, regions of rapid calcification (e.g. branch tips of *A. yongei*) may only have an oral and aboral ectoderm (Jokiel 2011).

A coral colony is comprised of genetically identical individuals, polyps, that are connected along the surface of the colony by a skin, the coenosarc, and by a shared gastrovascular network, the coelenteron (Fig. 1). The coelenteron comes in contact with the surrounding seawater through mouths at the center of each polyp and contains a fluid that is different in composition from seawater. The fluid functions as a vehicle for nutrient exchange, waste excretion, and the uptake of *Symbiodinium* algae (addressed below) (Tresguerres et al. 2017). Coral polyps' mouths are surrounded by tentacles that capture plankton from seawater.

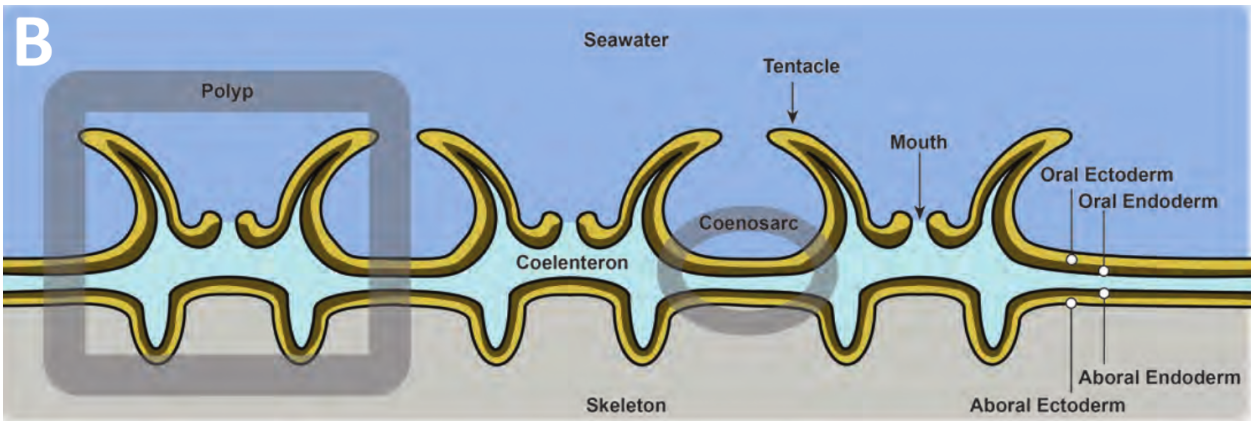

Figure 1. From Tresguerres et al. 2017. Diagram of three polyps of a coral colony above their skeleton. Polyps are connected by a skin (coenosarc) and a gastrovascular network (coelenteron).

Some of the gastrodermal cells of scleractinian corals contain symbiotic dinoflagellate algae of the genus *Symbiodinium*. The algae are hosted intracellularly within a coral-derived membrane envelope, the symbiosome membrane. Host cells typically contain only one alga but may occasionally contain up to three simultaneously. A single coral colony can also host multiple clades of *Symbiodinium* at any given time and experience changes in their ratios temporally. Some studies have demonstrated that different strains may confer increased resistance to thermal stress and may require different metabolic needs thereby hindering our ability to accurately assess the future of coral systems (Cunning et al. 2015a, Cunning et al. 2015b).

In contrast to anatomy, knowledge of basic coral cell biology is strikingly scarce. This lag in understanding is due in part to the low availability of experimental tools and resources. For example, the first *draft* coral genome (*Acropora digitifera*) was only recently sequenced (Shinzato et al. 2011) and long-term cell cultures and gene-manipulation techniques (e.g. siRNA, morpholino, CRISPER-Cas9) have not yet been optimized for coral research. This is due to our current inability to procure a viable supply of actively dividing cells and obtain coral embryos when not in the field. Coral's long development time additionally complicates the outlook for future use of these

techniques even if viable cell culture methods are perfected. One alternative approach is to use related Cnidarian species as model systems, for example the anemones *Aiptasia ssp.* and *Nematostella ssp.* (Gates et al. 1992, Weis et al. 2008). While these species do possess intracellular algal symbionts like reef-building corals, they do not calcify however, therefore limiting comparisons between model and coral systems.

Cell subtypes and tissue layer functions

Corals have many cell subtypes (Fig. 2); however, the physiological functions of each cell subtype and potential species-specific differences remain only partially characterized.

A *typical* oral ectoderm contains nematocysts, pigment cells, ciliated support cells with abundant microvilli, mucocytes, neurons, and epitheliomuscular cells (Goldberg 2002a). Many cells in the oral tissues are rich in green fluorescent proteins (GFPs) which is believed to protect the animal from harmful ultraviolet radiation and oxidative stress. Nematocysts, epitheliomuscular cells, and ciliated support cells are also involved in predatory feeding at the mouths of polyps. A diverse mucus-associated microbiome exists atop this layer and is believed to be involved with nutrient cycling including nitrogenous compounds, amino acids and organic acids (Chimetto et al. 2008, Krediet et al. 2013, Raina et al. 2010). Microvilli serve to increase surface area of the oral ectoderm and stir the surface boundary layer thus aiding in nutrient exchange with the mucus microbiome. Recent work suggests that some cyanobacteria may be abundant in surface mucus and oral tissue layers; given their role in fixing nitrogen, they may play an important role in host functioning (Lesser et al. 2014). Other studies have shown that microbes are present in all tissue layers of the coral animal and the term

'holobiont' now refers to the complete assemblage of organisms associated with the coral colony (e.g. *Symbiodinium*, bacteria, archaea, viruses, fungi) (Rohwer et al. 2002).

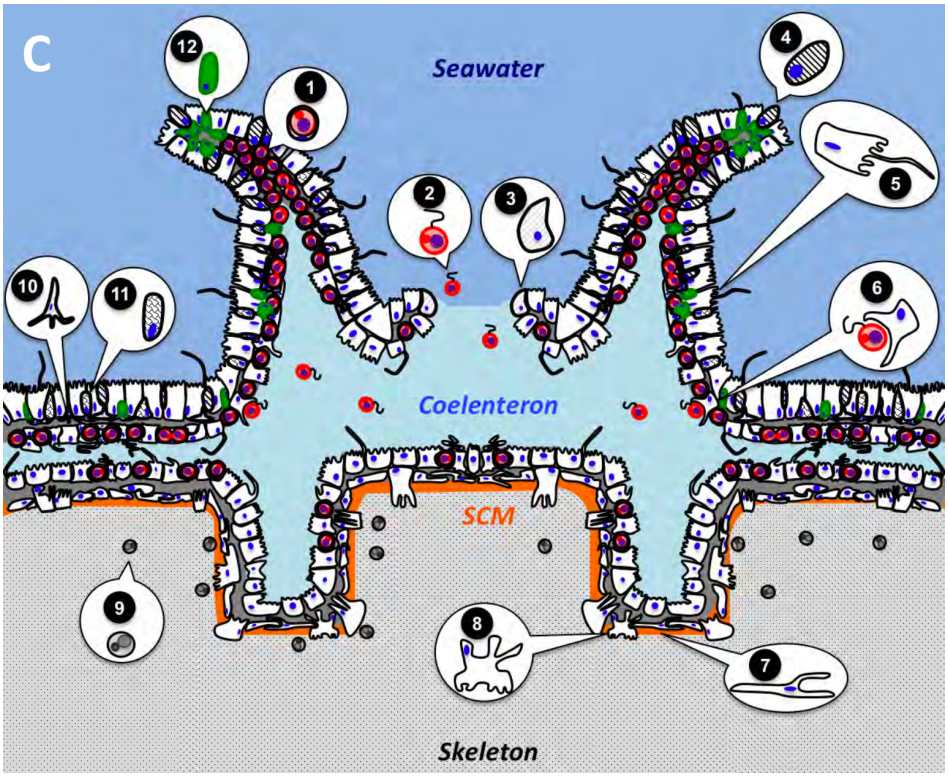

Figure 2. From Tresguerres et al. 2017. Cytology of a coral polyp. (1) Symbiotic *Symbiodinium* dinoflagellate in the symbiosome of a coral oral endodermal cell. (2) Free-swimming Symbiodinium. (3) Epitheliomuscular cell. (4) Nematocyst. (5) Ciliated support cell. (6) Endodermal cells in the process of phagocytosis of a Symbiodinium. (7) Calicoblastic cell. (8) Desmocyte. (9) Dead Symbiodinium incorporated into the skeletal matrix. (10) Neuron. (11) Mucocyte. (12) Pigment cell. Subcalicoblastic medium (SCM). Note: this is an artistic rendition used for illustrative purposes and does not accurately reflect cell sizes, morphology, relative proportions, or species-specific differences.

The oral and aboral endodermal layers are characterized by an abundance of *Symbiodinium*-hosting cells (Fig. 2). This symbiosis is essential for coral biology as *Symbiodinium* can produce up to 95% of fixed-carbon used for energy in corals (Davy et al. 2012). *Symbiodinium* also possess photosynthetic pigments that give corals their green-brown coloration under visible light and a distinctive red color with epifluorescence microscopy. The symbiosis is a dynamic process and can be gradually terminated under periods of stress if necessary. Certain conditions, such as prolonged ocean warming, can trigger mass expulsions of *Symbiodinium*; this phenomenon is

known as coral bleaching. Given its importance to coral biology and this thesis, photosynthesis and the *Symbiodinium*-coral symbiosis will be discussed further in a following section.

The coelenteron is a gastrovascular cavity in between the oral and aboral endoderms. The coelenteron fluid is circulated throughout the colony (Agostini et al. 2011) and displays a markedly different composition than seawater. For example, certain nutrients (e.g. vitamins, nitrogenous compounds, and PO_4^{3-}) can be up to 2,000-fold higher in the coelenteron (Agostini et al. 2011). The coelenteron fluid also exhibits highly variable levels of pCO_2, HCO_3^-, CO_3^{2-}, pH, and pO_2 that follow diel trends in response to photosynthesis, food digestion, and calcification (summarized in Table 1). Species-specific differences in coelenteron characteristics have also been observed. For example, coelenteron pH ranges from 8.5-7.5 for *S. pistillata* and 7.25-6.6 for *Galaxea fascicularis* during light and dark conditions respectively (Furla et al. 2000, Agostini et al., 2011). The true extent of these species-specific differences remains obscured by differing environmental conditions (light and nutrient levels), sampling season, and measurements techniques.

Table 1. Summary of dissolved inorganic carbon and calcium species composition of the coelenteron in *S. pistillata* over a diel cycle. Data obtained from Kühl et al. 1995, Furla et al. 1998, and Furla et al. 2000.

	Dark	**Light**
pH	7.5	8.5
Total DIC (mmol/L)	2.29	1.29
[HCO_3^-] (mmol/L)	2.17	1.02
[CO_3^{2-}] (µmol/L)	57	268
[CO_2] (µmol/L)	66	3
Aragonite oversaturation (%)	79	372
Calcite oversaturation (%)	143	672

The coral aboral endoderm remains the least characterized tissue layer both in terms of cytology and physiological roles. As this tissue layer lies between the coelenteron and the skeleton, it likely also plays a role in transporting dissolved inorganic carbon (DIC) and Ca^{2+} for calcification, nutrients for energy metabolism of calicoblastic cells, and in excreting waste products such as protons (H^{+}) (Fig. 2) (Tresguerres et al. 2017). The aboral endoderm may also contain some *Symbiodinium*-hosting cells that likely serve a similar function to the oral endoderm.

The aboral ectoderm is the interface between the coral animal and its $CaCO_3$ skeleton. It contains at least two cell types, desmocytes and calicoblastic cells, which are implicated in formation and maintenance of the skeleton. Desmocytes additionally anchor the living tissue to the skeleton (Goldberg 2001b). In between the aboral ectoderm and the skeleton is the subcalicoblastic medium (SCM), a highly alkaline fluid hypersaturated with respect to aragonite and potentially filled with excreted protein (Tresguerres et al. 2017, Mass et al. 2013, Mass et al. 2016).

Finally, the $CaCO_3$ skeleton lies below the living tissue layers in the form of an aragonite crystal lattice (Wainwright 1964). Porosity of the skeleton varies greatly by clade, colony morphology, and environmental conditions (Fantazzini et al. 2015). Organic components such as dead *Symbiodinium*, collagen and acid-rich proteins, lipids, and polysaccharides are also found in the skeleton (reviewed in Johnston 1980, Drake 2015). Previous studies determined organic content was much lower in abundance than aragonite but did not differentiate between freshly built and older skeleton; it is likely that organic content is higher in the freshly deposited skeleton. This collection of aragonite and organics is referred to as the skeletal organic matrix (SOM).

A variety of endolithic organisms have also been described in coral skeletons including cyanobacteria, fungi, bacteria, boring worms, and sponges further complicating the perceived role of the coral holobiont in whole-animal functioning. Given its importance to coral biology and this thesis, the process of coral calcification will be discussed further in the following section.

Calcification: the SCM, DIC transport, and Ca^{2+} transport

The following equilibrium equations are relevant to general coral biology (DIC equilibria, calcification, photosynthesis), to the following sections, and to the specific interests of this thesis:

i. DIC equilibria in water: $CO_2 + H_2O \Leftrightarrow HCO_3^- + H^+ \Leftrightarrow CO_3^{2-} + H^+$
ii. $CaCO_3$ formation/calcification: $Ca^{2+} + 2\ HCO_3^- \Leftrightarrow CaCO_3 + 2\ H^+$
iii. Photosynthesis: $6\ CO_2 + 12\ H_2O + Light \Leftrightarrow C_6H_{12}O_6 + 6\ O_2$
iv. Ammonia/ammonium equilibria in water: $NH_3 + H^+ \Leftrightarrow NH_4^+$

Skeletal formation in corals involves can be broken down into two key phases: (1) the precipitation of amorphous $CaCO_3$ and (2) its deposition as highly-structured aragonite crystals into the SOM. $CaCO_3$ precipitation requires specific physiological conditions namely high pH, high $[Ca^{2+}]$, and a high [DIC] (Eq. 1, Eq. 2, Fig. 3). To achieve conditions for optimal skeletal growth, corals maintain a strictly controlled region between the skeleton and aboral ectoderm: the SCM (Fig. 2). This jelly-filled space is markedly alkaline as to promote HCO_3^- and CO_3^{2-} speciation and CaCO3 deposition. It also contains excreted coral acid-rich proteins (CARPs) which can catalyze $CaCO_3$ precipitation even at pH ~7.1 (Mass et al. 2013). SCM pH has been observed to vary across diel cycles (pH ~8.7-9.3 and ~8.1-8.4 in daylight and nighttime hours respectively) and between species, but always remains in an aragonite saturation state favorable for calcification (Al-Horani et al. 2003, Venn et al. 2011). In contrast, the

cytoplasmic pH (pH_c) of calcifying cells remains at a constant ~7.4 (Venn et al. 2011) demonstrating that calcifying cells can excrete DIC and Ca^{2+} and remove H^+ against SCM concentration gradients all while maintaining intracellular pH (Tresguerres et al. 2017).

Current understanding of cnidarian calcification indicates that HCO_3^- is the DIC species delivered to calcifying cells and that it originates from metabolic CO_2 (70-75%) and seawater (25-30%) (Zoccola et al. 2015, Allemand et al. 2011, Furla et al. 2000). Metabolic CO_2 is produced during mitochondrial respiration and can be rapidly hydrated by carbonic anhydrase (CA) into HCO_3^- and H^+. HCO_3^- could then be moved to the site of calcification while H^+ is exported back towards the coelenteron. The discoveries of abundant mitochondria in calicoblastic cells (Barott et al. 2015a) and a family of coral HCO_3^- transporters (Slc4) (Barott et al. 2015b, Zoccola et al. 2015) further this theory. Slc4 proteins have been implicated in HCO_3^- delivery to the SCM for both *A. yongei* (Barott et al. 2015b) and *S. pistillata* (Zoccola et al. 2015) suggesting a conserved role in both the Complex and Robust clades. In both species, the Na^+/K^+ ATPase (NKA) colocalizes with Slc4 proteins along the basolateral membrane of calicoblastic cells and appears to energize the transport of HCO_3^- (Barott et al. 2015b).

Ca^{2+} must also reach the SCM for coral calcification, however, the mechanisms for Ca^{2+} transport are also not well-understood. Models for transcellular movement via ion transporters (Allemand et al. 2004), transcellular movement via vesicles (Mass et al. 2017), and paracellular movement (Jokiel 2011, Tambutté et al. 2011) have all been suggested. However, those mechanisms are not mutually exclusive and the cellular mechanisms for calcification likely involve contributions from multiple pathways.

Evidence exists for a role of Ca^{2+} channels in at least one tissue layer of *S. pistillata*: a L-type voltage-dependent Ca^{2+} channel was localized to the oral and aboral ectoderms suggesting uptake from seawater and export into the SCM (Zoccola et al. 1999). However, high concentrations of cytoplasmic Ca^{2+} are known to be toxic so sequestration in vesicles would be necessary if transporting concentrations relevant for calcification. More recently, amorphous calcium carbonate nanoparticles were found forming in calicoblastic vesicles before excretion into the SCM in *S. pistillata* (Mass et al. 2017). While other pathways could contribute to Ca^{2+} delivery, vesicular transcellular movement presents as a likely calcification strategy for *S. pistillata*, a coral in the Robust clade. More research is needed to determine if Complex corals exhibit a similar pathway.

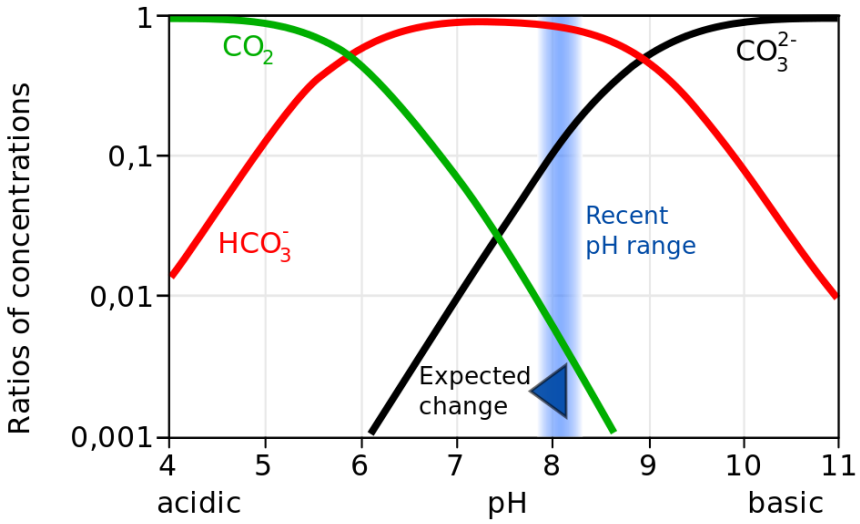

Figure 3. Taken from Wikipedia Commons (Carbonate_Sytem_of_Seawater.svg). Equilibria of aqueous DIC species in a Bjerrum plot. Species include carbon dioxide (CO_2), bicarbonate (HCO_3^-), and carbonate (CO_3^{2-}). Abundances are governed by the pH-dependent reaction $CO_2 + H_2O \Leftrightarrow HCO_3^- + H^+ \Leftrightarrow CO_3^{2-} + H^+$. Acidic conditions favor CO_2 formation while neutral and basic favor HCO_3^- and CO_3^{2-} formation respectively. The blue band depicts current ambient seawater pH (~8.1) with the arrow indicating the expected change with increased CO_2 emissions.

Calcification: light-enhanced calcification

A stimulatory effect of algal photosynthesis on calcification rates has long been observed in corals (Kawaguti 1937), which was named “light-enhanced calcification” and appears to be a nearly universal phenomenon in corals (reviewed in Allemand et al. 1998). In *S. pistillata,* for example, skeletal calcium incorporation increases four-fold in light vs. dark conditions (~80 nmol/mg protein and ~20 nmol/mg protein respectively) (Furla et al. 2000). Similarly, the aragonite saturation state of the SCM increases from 3 at night to 30 during daylight hours in multiple species (Al-Horani et al. 2003, Venn et al. 2011). The exact physiological mechanisms behind light-enhanced calcification are still unknown. Possible photosynthetically-stimulated mechanisms to drive calcification include increased: (a) carbohydrate production for use in energy metabolism, (b) O_2 production for aerobic respiration, (c) SOM precursor production, and (d) removal of calcification waste products including CO_2, H^+, PO_4^{3-} and NH_4^+ (reviewed in Allemand et al. 2011 and Tresguerres et al. 2017). Further studies are necessary to elucidate the mechanisms of coral calcification and nutrient exchange mechanisms between *Symbiodinium* and coral hosts.

Photosynthesis: *Symbiodinium*-coral relationship

Symbiosis with *Symbiodinium* is a common physiological strategy in the phylum Cnidaria being employed by both hard and soft corals, anemones, some jellyfish, and hydrocorals (reviewed in Davy et al. 2012). In corals, the symbiosis begins with an endocytosis event resulting in the formation of the symbiosome, a space enclosed by a host-derived membrane that contains the alga (Fig. 4). Under high magnification it is apparent that the host cell tightly encases the alga and the coral cytoplasm and

organelles are just barely visible (Kawaguti 1964, Barott et al. 2015b). The symbiosome membrane is modified following endocytosis to mediate the exchange of various compounds (discussed further below). The exact architectural changes made are still largely unknown however, it is accepted that the molecular composition and electrochemical properties of the symbiosome space are influenced both by host and *Symbiodinium*.

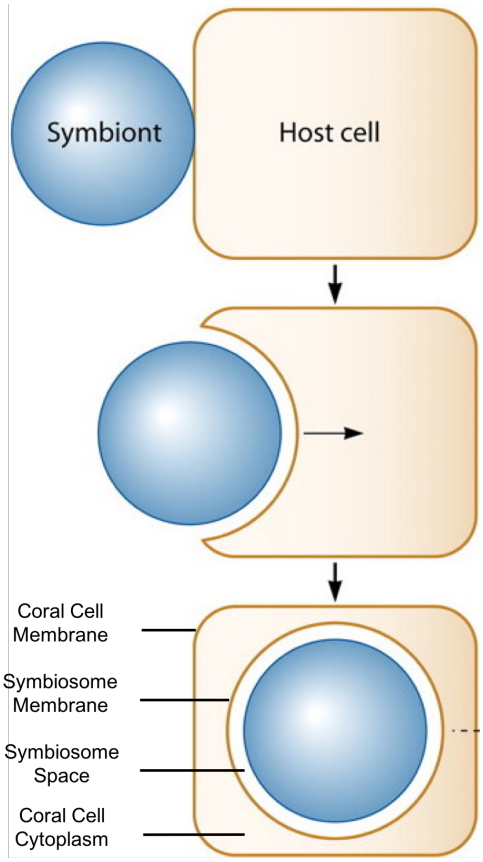

Figure 4. Modified from Davy et al. 2012. Formation of the coral-*Symbiodinium* symbiosis by phagocytosis. Each Symbiodinium is always partitioned from the host's cytoplasm by a plasma membrane. Successful endocytosis results in the separation and formation of a symbiosome membrane and a symbiosome space surrounding the alga.

Photosynthesis: the symbiosome

The symbiosome is the algae microenvironment and the interface for metabolic exchange between the alga and the host. The symbiosome membrane facilitates and regulates the transport of various metabolites including DIC, nitrogenous compounds,

amino acids, phosphates, and carbon compounds (Barott et al. 2015b, Pernice et al. 2012, reviewed in Davy et al. 2012). The symbiosome is markedly acidic with pH ~4 in both *A. yongei* and *S. pistillata* (Barott et al. 2015a). This very acidic pH is maintained by VHA, a proton pump that uses the energy from adenosine triphosphate (ATP) hydrolysis to move H^+ across cellular membranes against their electrochemical gradient (Cidon & Nelson 1983). VHA is abundantly expressed in the symbiosome membrane of corals from both the Robust and Complex clades, pointing to a conserved physiological role in the *Symbiodinium*-coral symbiosis. Pharmacological inhibition of coral VHA resulted in a pH increase of ~1 unit, and a reduction in algal O_2-production by ~30% in *S. pistillata*, and by ~80% in *A. yongei* (Barrot et al. 2015a). Those results suggested VHA is part of a carbon concentrating mechanism (CCM) for *Symbiodinium* photosynthesis.

Given that gases diffuse across cell membranes following partial pressure gradients, the only mechanism to concentrate CO_2 is to hydrate it into H^+ and HCO_3^-, move these dissolved ionic species across biological membranes, and then dehydrate them back into CO_2. The coral-driven CCM therefore must possess machinery to concentrate DIC species prior to CO_2 formation in the symbiosome space. Venn et al. 2009 measured the cytoplasmic pH of coral gastrodermal cells and determined that HCO_3^- would be the most abundant DIC specie. This finding suggests that corals would likely move HCO_3^- into the symbiosome space where it would dehydrate into CO_2 at pH ~4 and in an abundance of H^+ (Eq. 1, Fig. 3, Barott et al. 2015a). While the protein(s) responsible for HCO_3^- movement are still unknown, VHA provides H^+ and might additionally provide the driving force for HCO_3^- movement. A model of this mechanism is

displayed in Fig. 5. Similar electrochemical gradients are used in a variety of cell types to energize the transport of water and a variety of ions (e.g. Ca^{2+}, Cl^{-}, PO_4^{2-}, SO_4^{2-}) and nutrients (e.g. amino acids, glucose, carbohydrates) (Palmgren & Nissen 2011, Blanco & Mercer 1998).

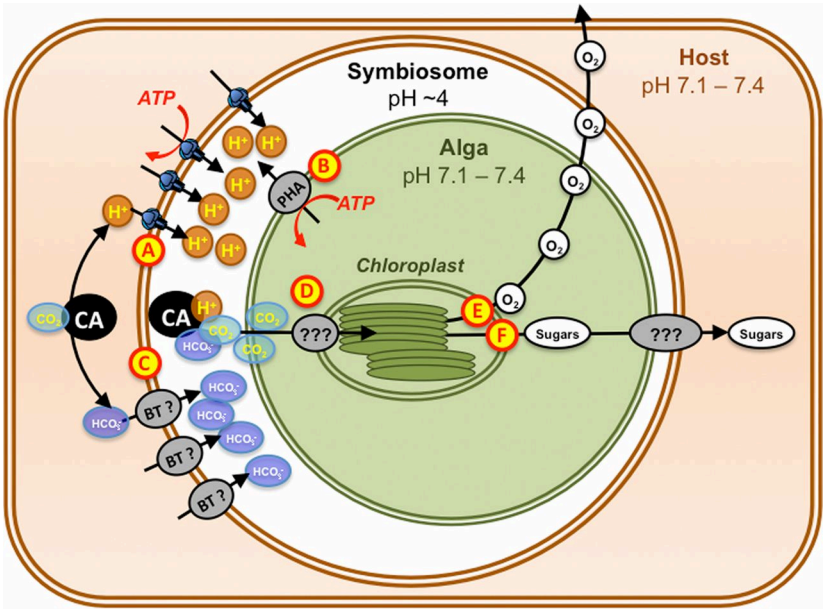

Figure 5. From Barott et al. 2015a. Model of the VHA-driven CCM in reef-building corals. H^+ enters the cell via VHA (A) and algal P-type H^+ ATPase (PHA) (B). HCO_3^- enters the symbiosome by a yet undescribed bicarbonate transporter (BT) (C). CA catalyzes the dehydration of HCO_3^- and H^+ into CO_2 which diffuses across the algal cell wall. Within the alga CO_2 is transported via unknown mechanisms to the sites of fixation (D). O_2 from photosynthesis diffuses out of the cell, across the symbiosome, and into the coral host (E). Sugars and other algal metabolites also enter the coral host via undescribed pathways (F).

Host-*Symbiodinium* metabolic exchange: delivery of nitrogen

Nitrogen is essential for algal metabolism and multiple studies have shown that free-living *Symbiodinium* experience natural nitrogen starvation in the water column (Cook et al. 1994). In contrast, those living in coral hosts are not nitrogen-limited (Grover et al. 2002) pointing to a coral-enhanced mechanism for nitrogen-delivery. While corals are known to generate large quantities of nitrogenous compounds, the mechanisms for their transfer are still unknown. These compounds, principally ammonia gas (NH_3) and ammonium ions (NH_4^+), originate from amino acid catabolism resulting

from predatory feeding on animals (Pernice et al. 2012, Eq. 4). At ambient 26°C and pH_c of 7.1-7.4, almost all NH_3 exists as protonated NH_4^+ ions (~97-99%) (Andrade & Einsle 2007, Weiner & Verlander 2017, Fig. 6). Given its prevalence in coral tissues, NH_4^+ appears an ideal candidate for a nitrogenous metabolite passed to *Symbiodinium*. A variety of findings back this assertion. First, NH_4^+ is the only reduced state of nitrogen that can be assimilated into biological molecules such as amino and nucleic acids via the glutamine synthesis pathway (Simon 2002, Voet et al. 2008). Second, *Symbiodinium* has been shown to preferentially uptake NH_4^+ over other nitrogenous compounds via the glutamine synthase pathway (D'Elia et al. 1983). Third, work using ion microprobe imaging observed rapid uptake and fixation of NH_4^+ by both *Symbiodinium* and coral cells following a seawater spike (Pernice et al. 2012). Finally, *Symbiodinium* fixed 14-23-fold more NH_4^+ than host cells in response to a seawater nitrogen spike (Pernice et al. 2012).

Importantly, acid-trapping mechanisms similar the CCM have been shown to drive NH_3/NH_4^+ movement across membranes in a variety of ssp. comprising plants, vertebrates, and invertebrates (Seckbach 2002, Wright & Wood 2009). When these findings are evaluated together, it suggests that coral host cells could selectively concentrate NH_4^+ in the symbiosome space via the electrochemical gradient established by VHA in a manner similar to the CCM.

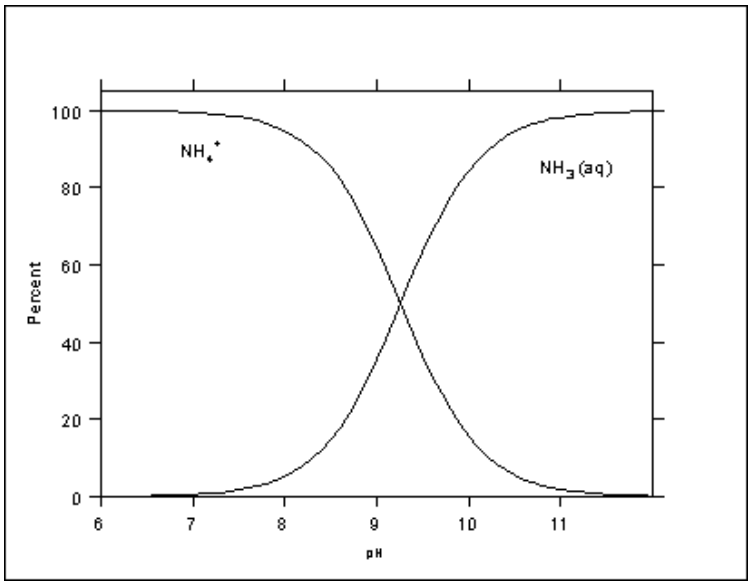

Figure 6. Taken from Illinois State Water Survey (nprop0{image7}.gif). Equilibria of aqueous ammonia (NH_3) and ammonium ions (NH_4^+) at 21°C. Abundances are governed by the pH-dependent reaction $NH_3 + H_2O \Leftrightarrow NH_4^+ + O_2$. Acidic conditions favor NH_4^+ formation while basic conditions favor NH_3 formation. At a pH_c of 7.1-7.4, ~97-99% will be in in the form of ionic NH_4^+ (Andrade & Einsle 2007).

Rh: an NH_3 gas channel

While NH_3 gas can diffuse across membranes following partial pressure gradients, biological systems have evolved gas channels to enhance diffusion and accelerate transport. NH_3 gas readily protonates at biologically relevant pHs to form NH_4^+ (Fig. 6). This ion is membrane-impermeable, thereby preventing backflow through gas channels, and must be moved by ion transporting proteins. The first NH_4^+ membrane transporter from *Escherichia coli* was sequenced in 1990 (Fabiny et al. 1990) and a number of specific families of transporters have been described since that time: (1) ammonium transport proteins (Amt) of bacteria, archaea, plants, and invertebrates, (2) methylammonium permeases (Mep) of yeast, and (3) Rhesus proteins (Rh) of animals. Mep, Amt, and Rh proteins often colocalize with other membrane transporters that establish electrochemical gradients such as VHA, H^+-K^+-ATPase, Na^+-H^+ exchangers (NHE), and NKA thereby driving the movement of NH_3/NH_4^+ (Masui et al. 2005, reviewed in Weiner & Verlander 2017). The exact mechanisms for action are

contested for Amts and Meps however, both function to import NH_4^+ into the cell cytoplasm (reviewed in Andrade & Einsle 2007).

The current consensus in literature is that Rh proteins act as conserved NH_3 gas channels that facilitate a net movement of NH_4^+ in vertebrates along NH_3 partial pressure gradients (Peng & Huang 2006, Weiner & Verlander 2017, Bourgeois et al. 2017). While NH_4^+ is the dominant species at biologically relevant pHs, some Rh proteins are believed to be capable of stripping the proton from NH_4^+ and conduct only NH_3 through an internal, hydrophobic channel while returning the H^+ to the original space (Baday et al. 2015). Once through the protein, NH_3 can recombine with a H^+ to form NH_4^+ (as reviewed in Andrade & Einsle 2007 and Khademi & Stroud 2006). In human kidney cells, while [NH_3] is ~100μM at a pH_c of 7.4, Rh proteins have been shown to result in a net NH_4^+ movement even when [NH_3] is only ~30μM in the kidney tubule (Gruswitz et al. 2010).

Rh: subgroups of the Rh family

Two main groups of Rh proteins have been described and both are named for their approximate molecular weight in kDa: Rh50s and Rh30s. Rh30 group proteins are usually non-glycosylated and have roles in immune and other functions (Huang et al. 2000). Glycosylated Rh50s comprise proteins commonly implicated in NH_3 transport and constitute a broader cohort with several subgroupings: RhA, RhB, RhC, RhD, Rhp1, and Rhp2 (RhA-D are often referred to as RhAG-AD in literature) (Huang & Peng 2005). RhA-Ds commonly occur in specific mammalian and vertebrate tissues and as such are generally well-characterized (Huang et al. 2000, Huang & Liu 2001, Baday et al. 2015). Rhp1-2 are the ‘primitive’ Rh proteins and are seen as ancestral to the

modern RhA-C clades (Huang 2008). Rhp1s occur in invertebrates and unicellular eukaryotes while Rhp2s are common in non-mammalian vertebrates (Huang & Peng 2005). Interestingly, all species with Rhp1 proteins also express Amt genes with the sole exception to this rule being vertebrates. Rhp groups are not well characterized and the mechanism behind NH_3 transport is not clear.

Rh: evidence for CO_2 transport

In addition, there is evidence from algae, slime mold, and mice for Rh proteins facilitating diffusion of CO_2 in conjunction with, or in place of, NH_3 (Kustu & Inwood 2006, Endeward et al. 2008, Musa-Aziz et al. 2009, Perry et al. 2010). This finding is supported by increased algal Rh expression levels in response to CO_2 addition (Soupene et al. 2002), decreased growth rate of alga at high CO_2 levels during RNAi knockdown of Rh (Soupene et al. 2004), no altered NH_4^+-sensing ability in slime mold during Rh disruption (Benghzal et al. 2001), and genetic ablation of a mouse Rh protein produced no phenotypes in renal ammonium excretion (Chambrey et al. 2005).

Rh: aquatic models for NH_3 excretion

Rh proteins are implicated in NH_3/NH_4^+ excretion for both fish and aquatic invertebrates illustrating their conserved evolutionary role across phyla (Thomsen et al. 2016, Wright & Wood 2009). Rh and H^+-excreting proteins often colocalize, establishing an electrochemical gradient favoring NH_4^+ excretion while preventing NH_4^+ from reentering the cell as NH_3 gas.

Aquatic vertebrate models for Rh-mediated NH_3/NH_4^+ excretion comprise freshwater and marine teleost fishes. In the gills of freshwater teleosts, a model for NH_4^+ excretion proposes NH_3 movement across Rh proteins is coupled with VHA activity that

provides a H^+ trapping mechanism for excretion (Wright & Wood 2009). Models for NH_4^+ excretion in marine teleosts notably disregard the potential role of VHA for H^+-trapping instead relying on NHEs to produce an H^+-rich boundary layer (Wilkie 2002); alternate models have suggested direct NH_4^+-Na^+ exchange via NHE isoforms or passive diffusion of NH_3 into seawater via Rh proteins (Wilkie 2002, Weihrauch et al. 2009).

Aquatic invertebrate models for Rh-mediated NH_3/NH_4^+ excretion also exist. In mytilid mussels, ciliary beating coupled with a Rh protein have been shown to enhance passive transport of NH_3/NH_4^+ across the gill epithelia (Thomsen et al. 2016). In seawater at pH 8, natural speciation to NH_4^+ prevents reabsorption and flushing of the gill epithelia prevented boundary layer saturation. VHA abundance in the gills increased at pH 8.5 as NH_4^+ speciation became less favorable; this upregulation potentially indicates an increased role of H^+ trapping in mussels at higher external pHs as passive diffusion of NH_3 becomes less efficient. Like in mussels, cephalopod gill epithelia are lined with Rh proteins but acidification to prevent NH_4^+ reabsorption is provided by NHEs instead of VHA (Hu et al. 2014). The decapod crab *C. maenas* has developed an alternative mechanism for transepithelial NH_3/NH_4^+ excretion: it is believed to concentrate NH_4^+ in intracellular acidic vesicles, which fuse to the apical membrane of gill cells thus releasing NH_4^+ to the surrounding water (Weihrauch et al. 2002). In this case Rh proteins together with VHA concentrate NH_3/NH_4^+ in the intracellular vesicles while additional transporters move NH_4^+ from the hemolymph into the epithelial cels (discussed below) (Weihrauch et al. 2018).

Other membrane transporters can potentially move NH_4^+

NH_4^+ has nearly identical biophysical characteristics to that of K^+ and as a result may act as a substrate for all K^+ transporters (reviewed in Weiner & Verlander 2017, Bergeron et al. 2003) such as NKA and K^+ channels. Most recently, the ancestral hyperpolarization-activated cyclic nucleotide-gated K^+ channel (HCN) was found to transport hemolymph NH_4^+ into branchial epithelial cells of the marine crab *Carcinus maenas* (Fehsenfeld & Weihrauch 2016b). Mammalian HCN2 has been demonstrated to move NH_4^+ (Carrisoza-Gaytán et al. 2011) but invertebrate HCN had only been implicated in olfactory signal transduction in the spiny lobster *Panulirus argus* (Gisselmann et al. 2005). Multiple studies have also shown the involvement of the Na^+/H^+ exchangers NHE3 and NHE4 in NH_4^+ movement; it remains unclear whether NHEs simply enhance the transfer of NH_4^+ by neighboring proteins or transport NH_4^+ in place of H^+ (Bourgeois et al. 2010, Kinsella & Aronson 1981). These recent findings complicate previous models and serve to illustrate our insufficient understanding of nitrogen transport in non-human systems.

Rh: potential role in the *Symbiodinium*-coral symbiosis, NH_4^+ excretion, and pH regulation

The limited knowledge on coral cell biology extends to nitrogen transport mechanisms and the presence and physiological roles of Rh proteins. Based on known physiological roles of Rh proteins in other aquatic animals, I hypothesize coral Rh plays roles in the following four key physiological mechanisms:

First, Rh proteins may facilitate the movement of NH_3/NH_4^+ from host cells to *Symbiodinium*. I hypothesize Rh works together with VHA in the symbiosome

membrane to trap NH_3 as NH_4^+ in the symbiosome. This putative nitrogen concentrating mechanism (NCM) would be akin to the mechanism of acid trapping found in freshwater teleosts, decapod crabs, and cephalopods, and would involve the localization of Rh together with VHA on the symbiosome membrane. The NCM would be analogous to the CCM for algal photosynthesis (Barott et al. 2016a).

Second, Rh proteins may play a role in nitrogenous waste excretion. I hypothesize that Rh may facilitate NH_3/NH_4^+ secretion across the apical membrane of the oral ectoderm into seawater. The lack of VHA along this membrane (Barott et al. 2015b) suggests that coral, like mytilid mussels, does not require NH_4^+ trapping at seawater pH 8 and might instead take place by passive NH_3 diffusion, possibly enhanced by stirring of the seawater boundary layer by apical microvilli in a similar manner to the ciliary beating of mussels (Thomsen et al. 2016).

Thirdly, Rh proteins may enhance SCM pH regulation by facilitating delivery of NH_3 to the SCM. As previously discussed, SCM pH varies by species and over diel conditions but typically ranges from ~8-9.3. The percent of total NH_3/NH_4^+ existing as deprotonated NH_3 at these conditions ranges from ~6% (pH 8) to ~55% (pH 9.3) and could act as a weak base to uptake free H^+ generated from calcification (pKa = 9.24). I hypothesize that Rh may be localized to cells forming the aboral ectoderm including calicoblastic cells and desmocytes.

Finally, a yet unexplored function of NH_4^+ in corals is its potential to induce protein precipitation and stabilization in extracellular compartments. In laboratory protein precipitation protocols, addition of NH_4^+ salts decrease protein solubility and induces precipitation; this process is deemed “salting-out” (Green & Hughes 1955). Salting-out

also tends to enhance the stability of native protein conformational folding by increasing the surface tension of water and shrinking the layer of water closely associated with the protein. This effect results in increased self-association of the protein (Wingfield 2016). NH_4^+ salts are ideal candidates for protein precipitation as they rapidly increase surface tension of water while remaining highly soluble. Low molecular weight proteins require higher salt concentrations to induce precipitation while large, and multiprotein complexes can be precipitated at <20% saturation (Wingfield 2016). Short of inducing precipitation, low concentrations of NH_4^+ can return denatured proteins to their original conformational folding state by increasing self-association and enhance structural stability (Mitchinson & Pain 1986). In short, low percent saturation of NH_4^+ can increase conformational stability of both individual proteins and large, multiprotein complexes.

Proteomic analyses of the SCM in *S. pistillata* revealed a suite of biomineralization-related proteins that act as an organic scaffold to shape $CaCO_3$ crystals (Drake et al. 2013, Ramos-Silva et al. 2013). NH_4^+ transport into this compartment may increase the stability and maintain the association of these complexes. The analysis also revealed smaller SOM proteins that are key to $CaCO_3$ crystal organization and incorporation into the skeleton (Drake et al. 2013). I propose, in coral, NH_4^+ may enhance the stability of multiprotein complexes in the SCM. Alternatively, higher [NH_4^+] may induce the precipitation of these proteins and their association with the skeletal-SCM interface. However, NH_4^+ levels in the SCM are unknown, probably due to the difficulty in accurately analyzing the composition of this thin compartment.

Thesis goals

The goal of this thesis is to provide a first characterization of the molecular and cellular mechanisms involved in nitrogen excretion and metabolic exchange between the coral animal and *Symbiodinium* with a specific focus on Rh proteins.

This study utilized molecular and immunohistochemistry techniques to: (a) clone *A. yongei* Rh (ayRh) and establish its phylogenetic relationship to other Rh homologs, (b) establish the cellular and sub-cellular localization of coral Rh, (c) explore potential changes of Rh sub-cellular localization in gastrodermal cells during diel cycles, and (d) investigate the potential role of Rh and VHA in generating a NCM to sustain *Symbiodinium* nitrogen metabolism. This study is the first to investigate a coral Rh protein and its potential role in metabolic exchange with *Symbiodinium*.

METHODS

Study animals

Colonies of *A. yongei* were obtained from Birch Aquarium in La Jolla, CA. Coral were maintained in 3 parallel flow-through aquaria with 25°C seawater at Scripps Institution of Oceanography. This species is native to the Indo-Pacific region but was raised in an aquarium setting. Lighting conditions were a 10hr/14hr light-dark cycle with dawn and dusk lighting preceding sunrise at 08:00 and following sunset at 18:00 by 15 minutes. Simulated moonlight followed dusk lighting for 4 hours at the beginning of the 14-hour dark period, provided by Orbit Marine LED Fixture model 4103-B lights on the preset M3 lighting program. Tanks were cleaned twice a week to remove algal buildup on aquaria or on coral stands. Specimens were allowed to acclimate for at least 3 days pre-sampling.

Cloning of Rh from *A. yongei*

Total RNA was obtained as previously described (Barott et al. 2017). cDNA was synthesized using SuperScript III Reverse Transcriptase (Invitrogen, Carlsbad, CA, USA) and oligo(dT) primers. RT-PCR was performed with primers designed against untranslated regions of a predicted A. digitifera Rh mRNA: FWD primer 5'-CCACAATTCCGTC-3', REV primer 5'-GTCCGAGACATCTTGCATACC-3' (35 PCR cycles, anneal temperature of 63°C, 1.5 min extension step, using Phusion High Fidelity polymerase (New England Biolabs, Ipswich, MA, USA). Additional PCR rounds using nested primers to further amplify cDNA followed: FWD primer 5'-AACGGCCGCCAGTGTGCTGGGTTCGCACTCGCTCCATATT-3', REV primer 5'-AGCGGCCGCCAGTGTGATGGATTTTCTTGATCTCGGCTTCACTC -3' (35 PCR

cycles, anneal temperature of 64°C, 1.5 min extension step, using Phusion High Fidelity polymerase). These primers encoded homology regions for pCR2.1-TOPO vector digested with EcoR 1 and EcoR V restriction enzymes. Bands were gel-purified (NucleoSpin kit, Macherey-Nagel, Düren, Germany) and cloned into the EcoR 1/V-digested pCR2.1-TOPO vector and sequenced (Retrogen Inc.). ayRh can be accessed on Genbank using accession number MH025799.

Amino acid sequences for the phylogenetic analysis were sourced from Huang & Peng 2005 and Genbank via BLAST search. Sequences were aligned using MUSCLE (Edgar 2004) and a maximum likelihood tree with 500 bootstraps was inferred by RAxML (PROTGAMMA model of rate heterogeneity, WAG substitution model). Prediction of transmembrane helices was performed using TMHMM (http://www.cbs.dtu.dk/services/TMHMM-2.0/) (Sonnhammer et al. 1998, Krogh et al. 2001).

Antibodies

A custom polyclonal antibody was developed in rabbits and affinity purified (GenScript USA, Inc.) against the peptide antigen HNKDAHGSHKEGSN. The peptide was designed against a region of a predicted coral Rh protein from the *A. digitifera* genome (Shinzato et al. 2011). The antibody was validated for use on *A. yongei* with Western blotting of tissue homogenates (Fig. 8) and with immunofluorescence microscopy on tissue sections (Fig. 9, Fig. 10) and isolated cells (Fig. 13).

A custom polyclonal rabbit antibody targeting the conserved VHA_B subunit was also employed (epitope AREEVPGRRGFPGY; GenScript USA, Inc.). This antibody was previously validated by Western blot and immunofluorescence microscopy

preabsorption controls (sections and cell isolations) in *A. yongei* as well as sharks and marine worms (Barott et al. 2015a, Tresguerres et al. 2010, Tresguerres et al. 2013).

Coral Rh protein expression

Live coral tissue was removed from the skeleton using an airbrush and homogenized as previously described (Barott et al. 2015b). Homogenate was then sonicated on ice for 4 x 10-second bursts with 1 minute of rest between. This crude homogenate was then centrifuged at 500 x g for 15 minutes at 4°C to pellet down cell debris; supernatant was saved and labeled “crude homogenate.” Sample protein concentrations were determined using a Bradford Protein Assay (Bio-Rad, Hercules, CA, USA). Homogenates were kept on ice but not frozen prior to denaturation. 4x Laemmli buffer (Bio-Rad) and 10% beta-mercaptoethanol were added to samples before heating at 90°C for 3 minutes. 22.5 µg protein were loaded into a 10% polyacrylamide SDS-PAGE gel in a Mini-Trans Blot Cell (Bio-Rad) with Running buffer (25 mM Tris, 190 mM glycine, 0.1% SDS). Electrophoresis was run for 100 minutes at 100 V and 4°C. 4 µl of Precision Plus Dual Color Protein Standards were also loaded (Bio-Rad).

Following electrophoresis, the gel was washed in distilled water ater for 5 minutes and equilibrated in Towbin buffer (25 mM Tris pH 8.3, 192 mM glycine, 20% (v/v) methanol) for 15 minutes. Proteins were transferred from the gel onto a PVDF membrane using a Mini Tans-Blot Cell overnight in Towbin buffer at 0.09 A and 4°C. PVDF membranes were washed in Tris-buffered Saline + 0.1% Tween detergent (TBS-T) for 15 minutes on a shaker at room temperature to remove excess transfer buffer

prior to blocking. Membranes were then blocked with 5% powdered fat-free milk in TBS-T for 1 hour on a shaker at room temperature.

Following blocking, membranes were incubated overnight on a shaker at 4°C with coral Rh primary antibody (0.216 µg/ml; 1:5000 dilution from 1.08 mg/mL stock), primary antibody with 400x excess peptide on a molar base ('pre-absorption control'), or pre-Immune Serum (0.216 µg/ml) diluted in blocking buffer. Membranes were then washed with 4 x 15-minute TBS-T washes prior to incubation with secondary antibody (goat anti-rabbit-HRP diluted 1:10,000, Bio-Rad) for 1 hour on a shaker at room temperature. Membranes were again washed with 4 x 15-minute TBS-T washes and a final 15-minute TBS wash prior to band development with a ECL Prime Western Blot Detection Kit (GE Healthcare, Chicago, IL, USA) and imaged using a Chemidoc Imaging system (Bio-Rad). Negative controls are presented in Fig. 8.

Coral Rh protein expression: protocol optimization

Optimization of the above Rh protein blotting protocol was a lengthy process that required manipulation of homogenization techniques, sample electrophoresis buffers, denaturation temperatures, transfer protocols, primary antibody concentrations, and wash steps. Frozen crude homogenate was originally used but was determined to cause protein degradation; following this discovery homogenates were prepared fresh each day. Sonication and the initial debris clean-up steps were also added following airbrushing to break down coral mucus. Multiple electrophoresis buffers were also used: 2x Laemmli buffer (Bio-Rad), 4x Laemmli buffer, and Fairbanks buffer (10 mM Tris-HCl, 1 mM EDTA, 5% sucrose, 1% SDS, 40 mM dithiothreitol (DTT), 10 µg/mL Pyronin Y). Denaturation temperatures were also varied for crude homogenate samples: on ice (15

minutes), room temperature (15 minutes), 37°C (15 minutes), 50°C (15 minutes), 70°C (15 minutes), 90°C (1, 3, 5, 20 minutes), and 100°C (1 and 5 minutes). Gel transfers to a PVDF membrane were originally carried out using TurboBlot transfer stacks and transfer buffer (Bio-Rad). This method was determined to poorly transfer larger proteins so overnight, 4°C wet transfers with Towbin buffer were employed instead. This method provided much-improved protein transfer especially when running buffer was rinsed from the gel and the gel was allowed time to equilibrate in Towbin Buffer prior to transferring. Primary antibody concentration was varied to optimize Rh:background signal ratio (1:1000, 1:2000, 1:4000, 1:5000, 1:10,000 in blocking buffer). The number and length of TBT- washes was also varied pre- and post-secondary antibody incubation (3 x 10-minute washes, 3 x 15 minute washes, 4 x 15 minute washes). A 15-minute TBS-T wash was also added prior to membrane blocking. Finally, a 15-minute 1X TBS wash was added immediately prior to imaging to remove Tween detergent. Additional resources including the Bio-Rad Protein Blotting Guide can be found online (http://www.bio-rad.com/en-us/applications-technologies/protein-blotting-methods).

Immunolocalization of Rh in coral tissues

Coral branches were fixed for immunohistochemistry and decalcified as previously described (Barott et al. 2015a, Barott et al. 2015b, Barott & Tresguerres 2015). Following decalcification, branches were dehydrated and embedded in sterile paraffin wax. Blocks were sectioned in 7-5 μm thick slices and floated with a drop of water on glass microscope slides. Slides were incubated on a 32°C hotplate overnight to allow for section adhesion prior to storage at 4°C until use. Sections were rehydrated and blocked for 1 hour at room temperature in blocking buffer (phosphate buffered

saline (PBS) with normal goal serum and keyhole limpet hemocyanin solution, pH 7.4). Overnight incubation at 4°C with coral Rh antibody (2.16 µg/ml in blocking buffer), with coral Rh antibody pre-absorbed with excess peptide (8.64 µg/ml in blocking buffer), or with pre-Immune Serum (2.16 µg/ml in blocking buffer). “Secondary-only” control images were incubated with blocking buffer overnight in place of coral Rh antibody. Slides were washed 3 times for 5 minutes in PBS with Triton-X (0.2%) (PBS-TX) the following morning to remove unbound Rh antibody. Secondary antibody solutions (goat anti-rabbit-Alexa Fluor555, 4 µg/ml; Invitrogen) were then added for 1 hour at room temperature. A 5-minute, room temperature incubation with Hoechst DNA Stain (1 µg/ml) followed. Finally, slides were again washed 3 times for 5 minutes in PBS-TX to remove unbound secondary antibodies. Slides were imaged using a fluorescence microscope (Zeiss AxioObserver). Negative controls are presented in Fig. 9 and Fig. 10.

Coral cell isolations were prepared for immunohistochemistry as previously described (Venn et al. 2009, Barott & Tresguerres 2015). Briefly. Coral fragments were cut, submerged in 0.2 µm filtered seawater, and gently brushed with a toothbrush to remove cells. Cells were pelleted from seawater with a 3,000 x g centrifugation for 4 minutes at 4°C. Cells were resuspended and fixed in S22 Buffer (450 mM NaCl, 10 mM KCl, 58 mM $MgCl_2$, 10 mM $CaCl_2$, 100 mM Hepes, pH 7.80) with 4% paraformaldehyde for 15 min on ice. Cells were again pelleted with a 3,000 x g centrifugation for 4 minutes at 4°C to remove fixative; cells were resuspended in a small volume (~500µL) of S22 buffer. Cells were then pipetted onto glass microscope slides and allowed to air dry at 4°C. Cells were allowed to dry no longer than 1 hour before being stained. Staining and negative controls were performed as described above. This method causes coral cells

to lose their polarity and flatten, but coral gastrodermal cells with *Symbiodinium* are still identifiable. Negative controls are presented in Fig. 13.

24-hour cell isolations to investigate Rh localization in algae-hosting cells

Coral cell isolations were prepared in triplicate over a 24-hour period. Colonies were chosen at random from the 3 aquaria. Samples were taken 30 minutes before and after sunrise and sunset (07:30, 08:30, and 17:30, 18:30 respectively) as well as halfway between light changes (13:00 & 23:00). Samples taken during light hours were continually illuminated during isolation and fixation while those taken during night hours were kept in the dark. Cells were stained for Rh at each time point (N=3) as well as VHA (3 µg/mL) at 13:00 and 2300 (N=1). Cells were observed and the subcellular localization of Rh was classified as predominantly (a) on the symbiosome membrane, (b) in host cytoplasm, or (c) unable to be determined. Symbiosome membrane localization was determined by observing clear, concentrated staining separating the nuclei of the host and the *Symbiodinium*. Cytoplasmic staining was classified as diffuse staining between nuclei and the absence of clear, concentrated staining. Cells with intermediate staining were classified as unclear. At each time point, the first 50 intact algae-hosting cells with both the algal and coral nuclei in the same focal plane were counted and classified. Only cells with signal were counted. Slides were counted in a double-blind manner to avoid bias.

Statistical analyses

All statistical tests were run with Prism 6. Data from Rh localization in cell isolates were arcsin-square-root-transformed prior to analysis (Wang & Douglas 1998,

Barott et al. 2013). Data normality were tested with a D'Agostino & Pearson omnibus normality test. A non-parametric Friedman test was used to analyze non-normal data.

RESULTS

ayRh gene sequence and protein structure

The open reading frame of the cloned ayRh transcript had 1440 base pairs. The encoded protein has a predicted molecular weight of 51.8 kDa and 12 transmembrane domains, similar to vertebrate Rh proteins. No evidence for splice variants or isoforms was found. NCBI BLAST searches in genomic and transcriptomic databases revealed orthologues from vertebrate and invertebrate groups including Robust and Complex corals. Phylogenetic analysis revealed that ayRh is grouped within the larger Rhp1 cluster and is most closely related to other predicted Cnidarian Rh proteins (Fig. 7). Limited by a lack of characterization of related Cnidarian proteins, these analyses suggest that ayRh is likely a conserved Rhp1-type NH_3 gas channel with structural and functional similarity to those of other invertebrate species.

Figure 7. Maximum likelihood cladogram of *A. yongei* Rh in relation to invertebrate and vertebrate Rh proteins. Rh family subgroups are highlighted: Rh30 (orange), RhA (yellow), RhB (red), RhC (cyan), Rhp1 (green), Rhp2 (magenta). Taxa names from the phylum Cnidaria are labeled in red and A.yongei in blue. Amino acid sequences were aligned using MUSCLE and a maximum likelihood tree was generated using RAxM (500 bootstraps, PROTGAMMA model of rate heterogeneity, WAG substitution model). The following accession numbers were used for obtaining predicted transcripts, mRNA, or protein sequences: *Acanthaster planci* (Crown of Thorns Starfish) (RhB: XP_022107421.1), *Acropora digitifera* (RhA: XP_015769291.1), *Acropora yongei* (Rh: MH025799), *Ambystoma tigrinum tigrinum* (Tiger Salamander) (RhA: AAV28818.1), *Anopheles darlingi* (Mosquitto) (Rh: ETN62951.1), *Bos taurus* (Cow) (Rh: NP_777137.1, RhA: NP_776596.1, RhB: NP_777148.1, RhC: NP_776597.1), *Branchiostoma belcheri* (Amphioxus) (RhA: XP_019645061.1), *Caenorhabditis briggsae* (Rh_1: XP_002636925.1, Rh_2: XP_002636585.1), *Caenorhabditis elegans* (Rh_1: AAF97864.1, Rh_2: AAF97865.1), *Callithrix jacchus* (Marmoset) (Rh: AAF22442.1), *Callorhinchus milii* (Ghostshark) (RhA: AFK10779.1), *Canis lupus familiaris* (Dog) (RhA: NP_001104238.1, RhB: NP_001003017.2, RhC_1: NP_001041501.1, RhC_2: NP_001041487.1), *Carcinus maenas* (Littoral Crab) (Rh: AAK50057.2), *Cebus capucinus imitator* (White Headed Capuchin) (RhA: XP_017354151.1), *Chlamydomonas reinhardtii* (Green Alga) (Rh_1: XP_001695464.1, Rh_2: AAM19665.1), *Crassostrea gigas* (Pacific Oyster) (RhB: EKC21768.1), *Danio rerio* (Zebrafish) (Rh50: NP_571622.1, RhA: NP_998010.1, RhB: NP_956365.2, RhC: AAM90586.1, RhD: NP_001019990.1), *Daphnia magna* (Daphnia) (Rh: KZS19566.1), *Dictyostelium discoideum* (Slime Mold) (Rh_1: XP_639042.1, Rh_2: XP_641341.1), *Drosophila pseudoobscura* (Drosophila) (Rh: AAV40852.1, Rh50: NP_001261434.1), *Exaiptasia pallida* (Brown Anemone) (RhA: XP_020893448.1, RhB: KXJ18310.1), *Gallus gallus* (Chicken) (RhC_1: NP_989798.1, RhC_2: NP_001004370.1), *Gorilla gorilla* (Gorilla) (RhA: NP_001266499.1, RhD: NP_001266526.1), *Homo sapiens* (Human) (RhA: AHY04440.1, RhC_1: NP_057405.1, RhC_2: P18577.2, RhD: BAR40328.1), *Lingula anatine* (Brachiopod) (RhB: XP_013381459.1), *Macaca mulatta* (Rhesus Macaque) (Rh: NP_001028136.3, Rh50: AAD13385.1, RhA: NP_001027987.1), *Metacarcinus magister* (Dungeness Crab) (Rh: AEA41159.1), *Mus musculus* (Mouse) (Rh30: AAC25123.1, RhB: AAF19371.1, RhC: AAF19373.1), *Nitrosomonas europaea* (Rh: AY377923.1), *Oncorhynchus mykiss* (Rainbow Trout) (RhA: AAP87367.1, RhC: NP_001117995.1), *Orbicella faveolata* (RhA: XP_020600999.1, RhB: XP_020601000.1, RhC: XP_020601001.1), *Oryctolagus cuniculus* (Rabbit) (RhB: NP_001075605.1), *Oryzias latipes* (Killifish) (Rh50: NP_001116374.1, RhB: NP_001098561.1), *Pan troglodytes* (Chimpanzee) (Rh: Q28813.2, RhA: NP_001009033.1, RhC_1: XP_016782540.1), *Papio anubis* (Baboon) (RhA: XP_003891396.1), *Pongo pygmaeus* (Orangutan) (Rh30: AAC94962.1, Rh50: AAG00305.1, RhC: XP_002825848.1), *Portunus trituberculatus* (Gazami Crab) (Rh: AHY27545.2), *Rattus norvegicus* (Rat) (RhB: NP_898877.1, RhC: NP_898876.1, RhD: NP_071950.1), *Saccoglossus kowalevskii* (Acorn Worm) (RhB: XP_006824549.1), *Salmo salar* (Salmon) (RhA: NP_001117044.1), *Sapajus apella* (Capuchin) (Rh30: AAF22501.1), *Squalus acanthias* (Dogfish) (RhB: AJF44128.1), *Sus scrofa* (Boar) (RhB: NP_999161.1, RhC: NP_999543.1), *Stylophora pistillata* (RhA: XP_022795555.1, RhB: XP_022795556.1), *Takifugu rubripes* (Japanese Pufferfish) (Rh30_1: NP_001027935.1, Rh30_2: AAU81656.1, RhA_1: NP_001027816.1, RhA_2: NP_001027817.1, RhA_3: NP_001032956.1, RhB_1: NP_001027818.1, RhB_2: NP_001027934.1), *Tetraodon nigroviridis* (Green Spotted Pufferfish) (Rh30: AAY41905.1, RhB: Q3BBX8.1, RhC: Q3BBX7.1), *Xenopus laevis* (Xenopus) (RhA: XP_018121493.1, RhB_1: NP_001011175.1, RhB_2: Q69D48.1, RhC_1: XP_012814245.1, RhC_2: Q5U4V1.1, RhD: NP_001084416.1). Sequences are sourced from Huang & Peng 2005 with additional sequences identified by NCBI BLAST search. Outgroup is the same used by Huang & Peng 2005. Scale bar represents an amount of genetic change of 2.0.

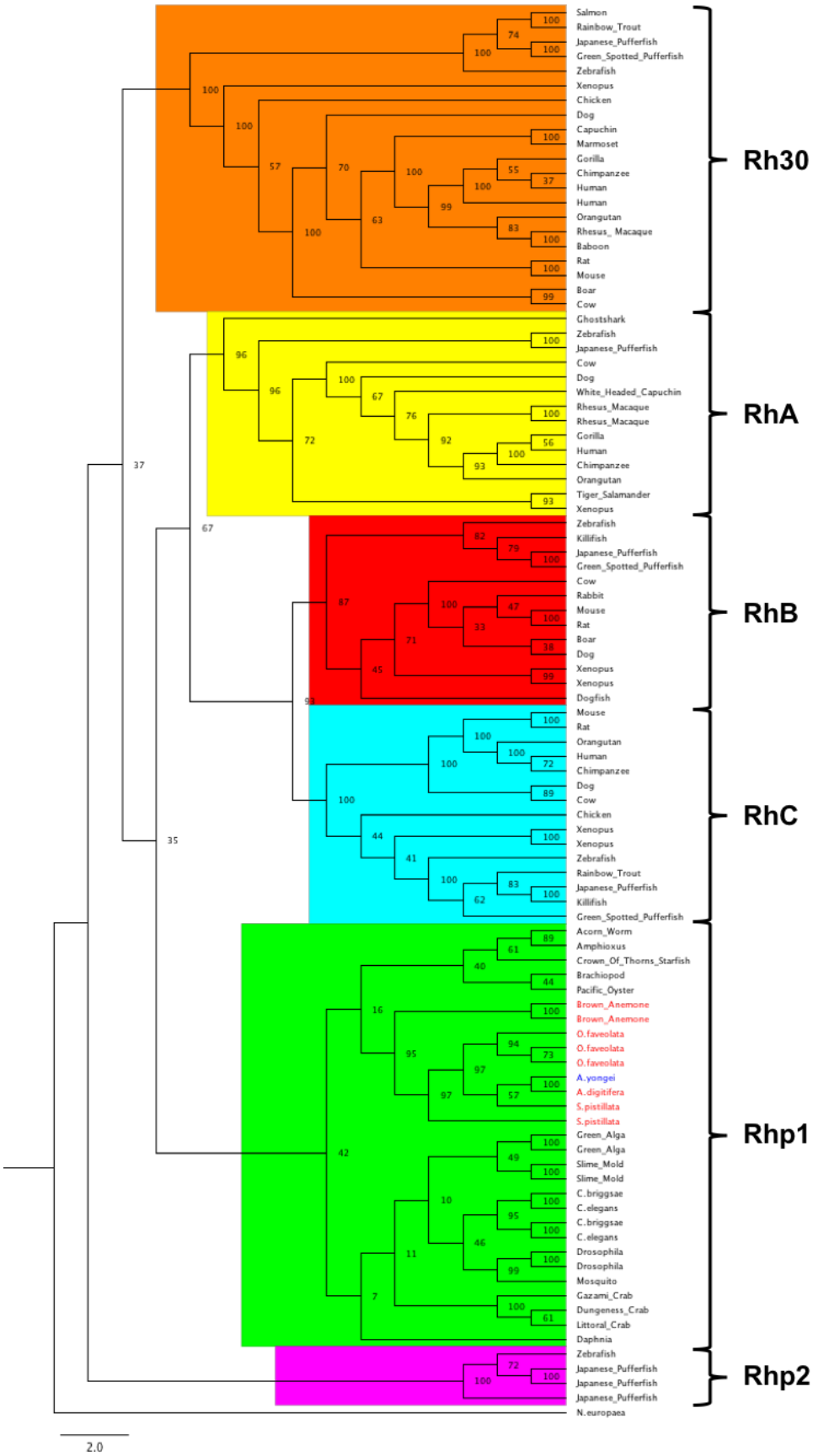
Salmon
Rainbow_Trout
Japanese_Pufferfish
Green_Spotted_Pufferfish
Zebrafish
Xenopus
Chicken
Dog
Capuchin
Marmoset
Gorilla
Chimpanzee
Human
Human
Orangutan
Rhesus_ Macaque
Baboon
Rat
Mouse
Boar
Cow
Rh30
Ghostshark
Zebrafish
Japanese_Pufferfish
Cow
Dog
White_Headed_Capuchin
Rhesus_Macaque
Rhesus_Macaque
Gorilla
Human
Chimpanzee
Orangutan
Tiger_Salamander
Xenopus
RhA
Zebrafish
Killifish
Japanese_Pufferfish
Green_Spotted_Pufferfish
Cow
Rabbit
Mouse
Rat
Boar
Dog
Xenopus
Xenopus
Dogfish
RhB
Mouse
Rat
Orangutan
Human
Chimpanzee
Dog
Cow
Chicken
Xenopus
Xenopus
Zebrafish
Rainbow_Trout
Japanese_Pufferfish
Killifish
Green_Spotted_Pufferfish
RhC
Acorn_Worm
Amphioxus
Crown_Of_Thorns_Starfish
Brachiopod
Pacific_Oyster
Brown_Anemone
Brown_Anemone
O.faveolata
O.faveolata
O.faveolata
A.yongei
A.digitifera
S.pistillata
S.pistillata
Green_Alga
Green_Alga
Slime_Mold
Slime_Mold
C.briggsae
C.elegans
C.briggsae
C.elegans
Drosophila
Drosophila
Mosquito
Gazami_Crab
Dungeness_Crab
Littoral_Crab
Daphnia
Rhp1
Zebrafish
Japanese_Pufferfish
Japanese_Pufferfish
Japanese_Pufferfish
Rhp2
N.europaea
2.0

ayRh protein expression in *A. yongei*

Western blotting confirmed the specificity of the anti-ayRh antibodies as well as expression of ayRh protein in *A. yongei* tissues. The anti-ayRh antibody recognized a ~52 kDa protein which matches predictions from the sequenced ayRh gene (Fig. 8). The antibody's epitope was 93% conserved in ayRh compared to the *A. digitifera* Rh protein that was for antibody design, with only one amino acid mismatch out of 14 (indicated in red and underlined) (*A. yongei*: HNKDAHGSPKEGSN, *A. digitifera*: HNKDAHGSHKEGSN). Peptide pre-absorption and rabbit pre-immune serum controls showed no signal at ~52 kDa nor any other weight. These results indicate that the antibody specifically recognizes ayRh. The anti-VHA antibody was previously validated for protein expression in *A. yongei* (Barott et al. 2015a).

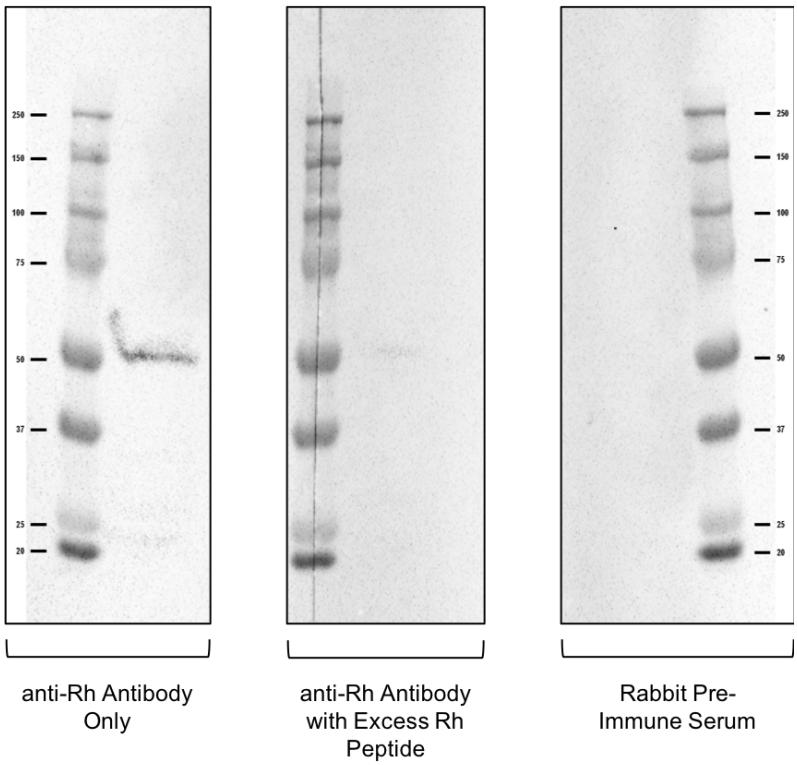

Figure 8. Immunoblot detection of Rh in *A. yongei*. The anti-Rh antibody recognizes a ~52 kDa protein which matches the predicted size of the sequenced *A. yongei* Rh gene. Peptide pre-absorption and rabbit pre-immune serum controls show highly-reduced and no signal indicating antibody specificity. Precision Plus Dual Color Protein Standards (BioRad) were used to determine relative protein molecular weights.

ayRh is localized to the oral ectoderm, desmocytes, and gastrodermal cells in sectioned *A. yongei* tissues

Immunofluorescence microscopy confirmed ayRh protein expression throughout *A. yongei* tissues, notably in the apical membrane of cells in the oral ectoderm, in a region of gastrodermal cells, and in desmocytes (Fig. 10, Fig. 11). Peptide pre-absorption and rabbit pre-immune serum controls greatly reduced or completely removed antibody staining in overall tissue sections (Fig. 9) (Fig. 10). The faint algal autofluorescence in the red channel remains visible in control images and is due to chlorophyll autofluorescence.

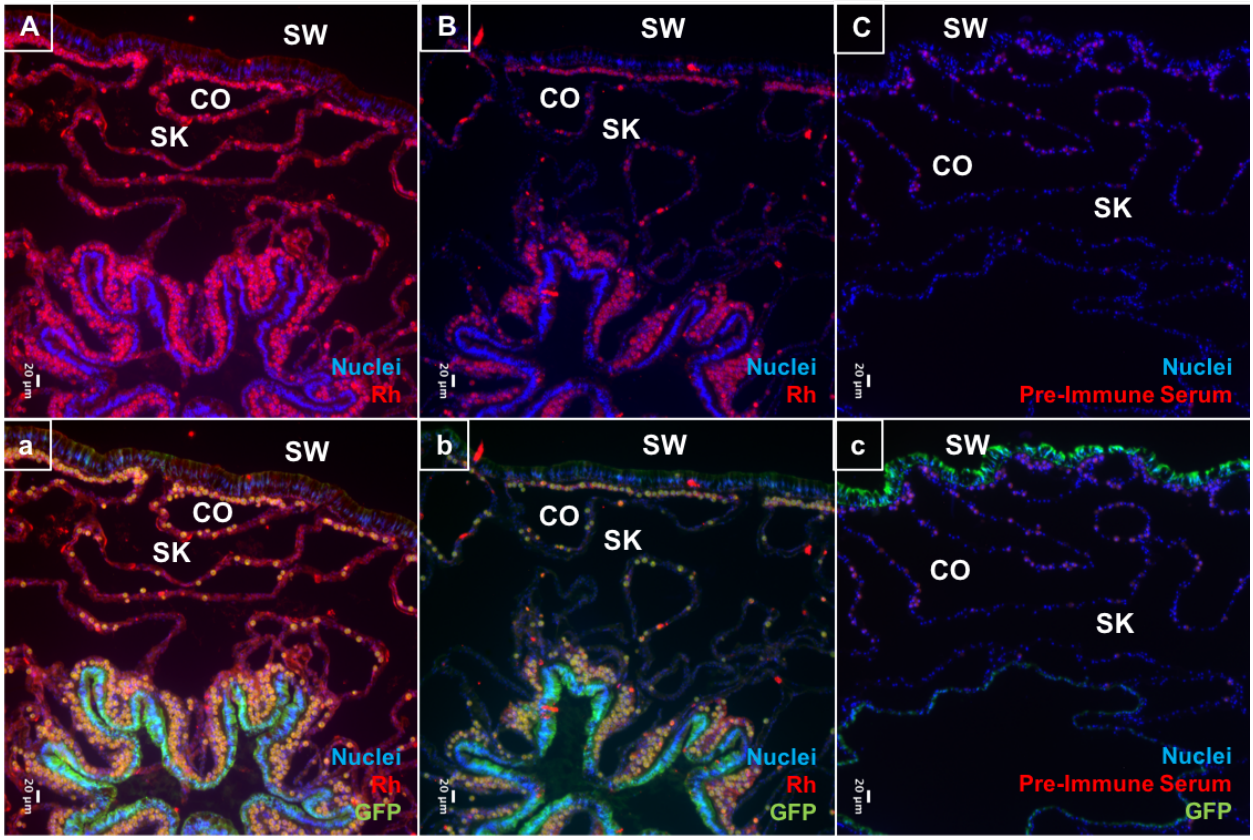

Figure 9. Overview image of Rh immunofluorescence microscopy controls in *A. yongei* tissue sections. (A & a) Anti-Rh antibody only, (B & b) peptide pre-absorption control, and (C & c) rabbit pre-immune serum control. Controls show reduction of red channel signal confirming antibody optimization. Algal autofluorescence in the red channel remains visible. Nuclei are labeled in blue, GFP in green, and Rh in red. Panels A-C show only nuclear and Rh staining while panels a-c include native GFP signal. SW: seawater, CO: coelenteron, SK: skeleton.

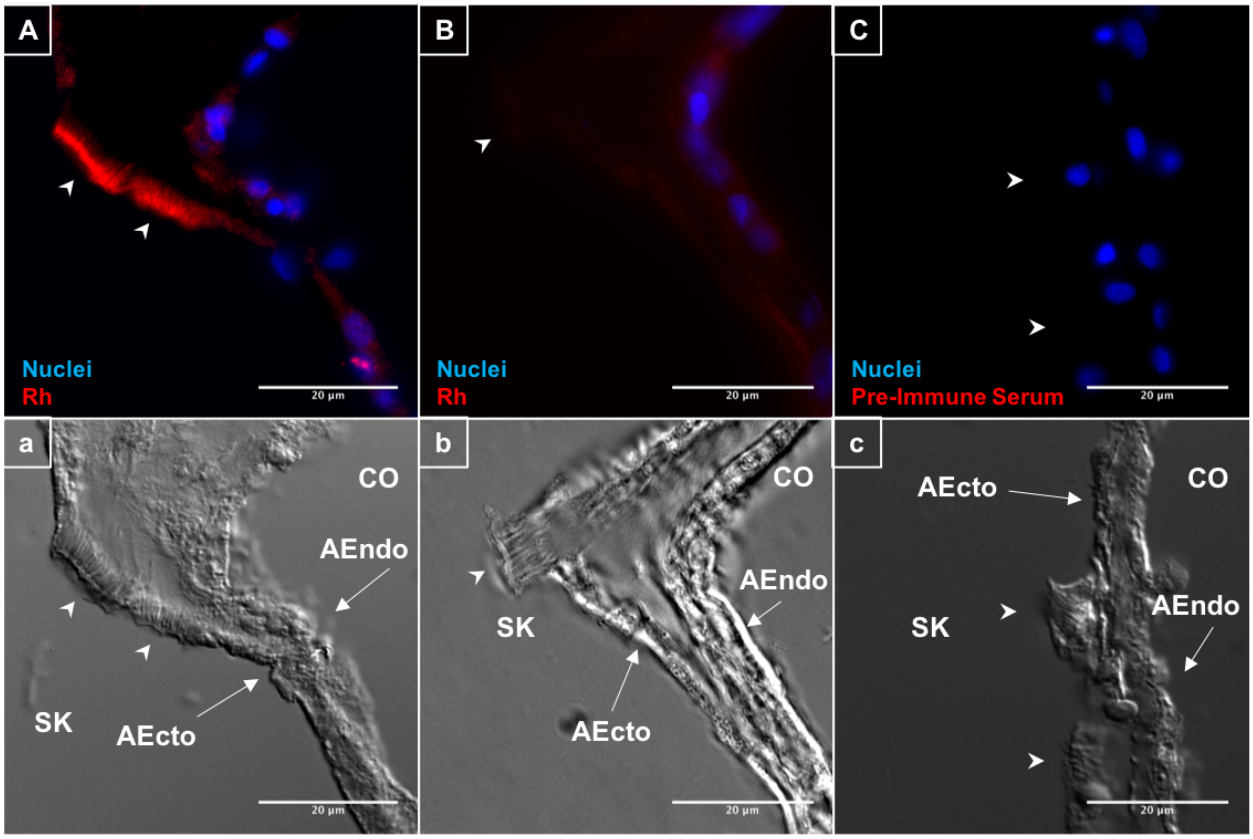

Figure 10. Rh immunofluorescence microscopy controls of desmocytes in *A. yongei* tissue sections. (A) Anti-Rh antibody only, (B) peptide pre-absorption control, and (C) rabbit pre-immune serum control. Nuclei are labeled in blue and Rh in red. Panels A-C show nuclear and Rh staining while panels a-c show accompanying DIC images to illustrate cell structure. Controls show reduction of red channel signal confirming antibody optimization. Algal autofluorescence in the red channel remains visible. Native GFP signal is not shown. White arrowheads show the apical membrane of desmocytes. CO: coelenteron, Aendo: aboral endoderm, Aecto: aboral ectoderm, SK: skeleton.

ayRh localizes to the apical and tenon boundary membranes of desmocytes

ayRh was consistently localized to desmocytes, cells that anchor living tissue to the skeleton. A transmission electron micrograph and illustration of this cell type is presented in Fig. 12 (adapted from Muscatine et al. 1997). Notably, the basolateral plasma membrane of desmocytes is profusely invaginated with the aboral mesoglea that separates the aboral tissue layers. These invaginations surround proteinaceous intracellular tenons that interdigitate with the mesoglea. Basolateral invaginations of the plasma membrane of desmocytes are thus referred to as tenon boundary membranes.

ayRh signal from desmocytes is very intense even at low magnification, indicating a high protein abundance (Fig. 11A box D). At high magnification, ayRh appears to localize to both the apical plasma membrane at the skeletal interface and along the tenon boundary with the desmocyte basolateral membrane; tenon boundary membranes are clearly identifiable as striations in both false color and DIC images (Fig. 10A/a, Fig. 11D/d). ayRh density on tenon boundary membranes appears to increase with proximity to the apical membrane.

Figure 11. Regions of Rh localization in *A. yongei* tissue sections determined by immunofluorescence microscopy. (A) Overview of an *A. yongei* branch showing regions of interest, (B) apical membrane of the oral ectoderm, (C) subcellular region of gastrodermal cells, and (D) apical membrane of desmocytes. (b-d) accompanying DIC images to illustrate cell structure. Nuclei are labeled in blue, native GFP signal in green, and Rh in red. Panel A includes native GFP signal while panels B-D include only nuclear and Rh staining. Algal autofluorescence in the red channel remains visible in panels B-D. SW: seawater, Oecto: oral ectoderm. Oendo: oral endoderm, CO: coelenteron, Aendo: aboral endoderm, Aecto: aboral ectoderm, SK: skeleton, M: mesoglea.

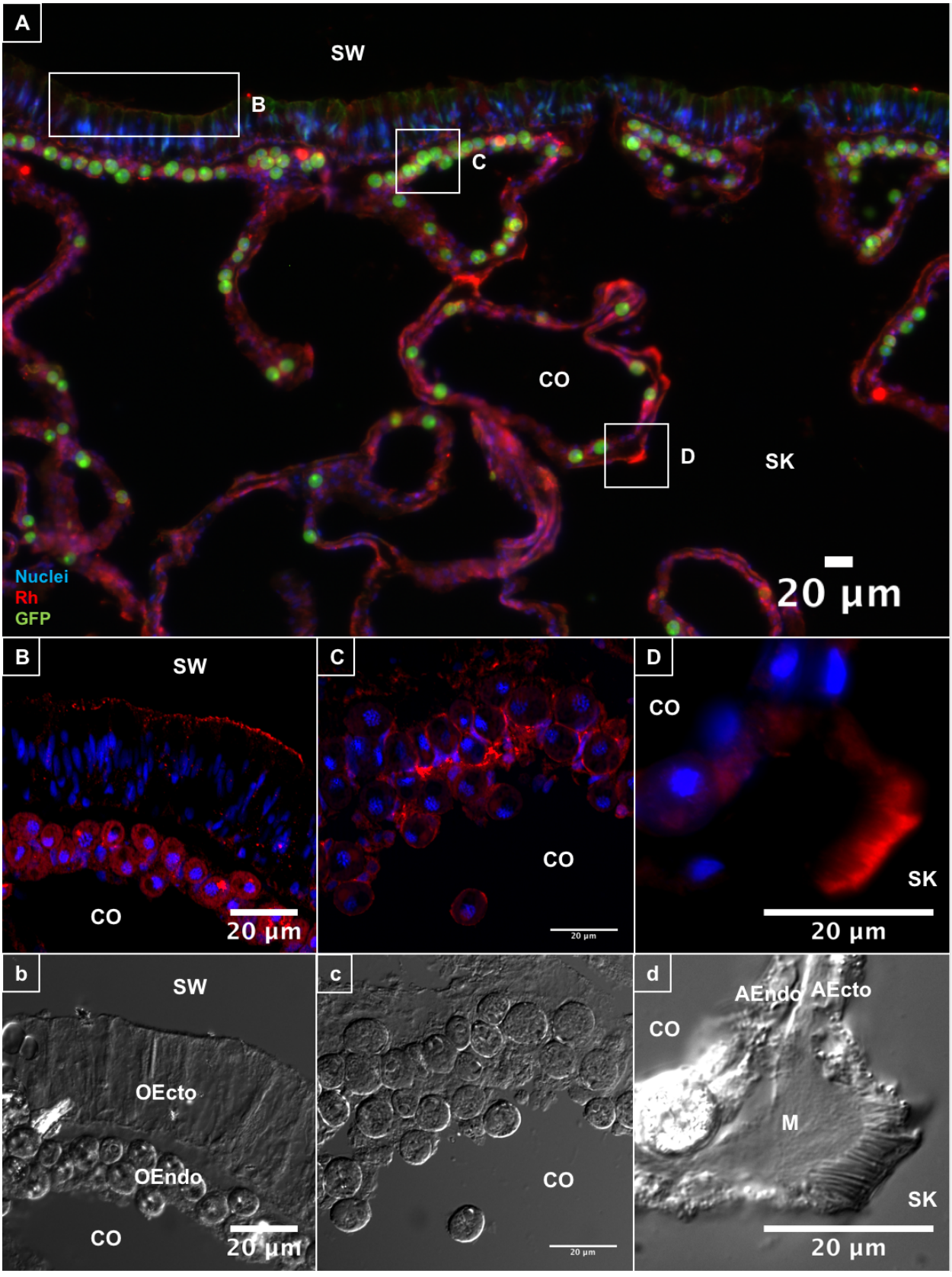
A
SW
B
C
CO
D
SK
Nuclei
Rh
GFP
20 µm
B
SW
CO
20 µm
C
CO
20 µm
D
CO
SK
20 µm
b
SW
OEcto
OEndo
CO
20 µm
c
CO
20 µm
d
AEndo
AEcto
CO
M
SK
20 µm

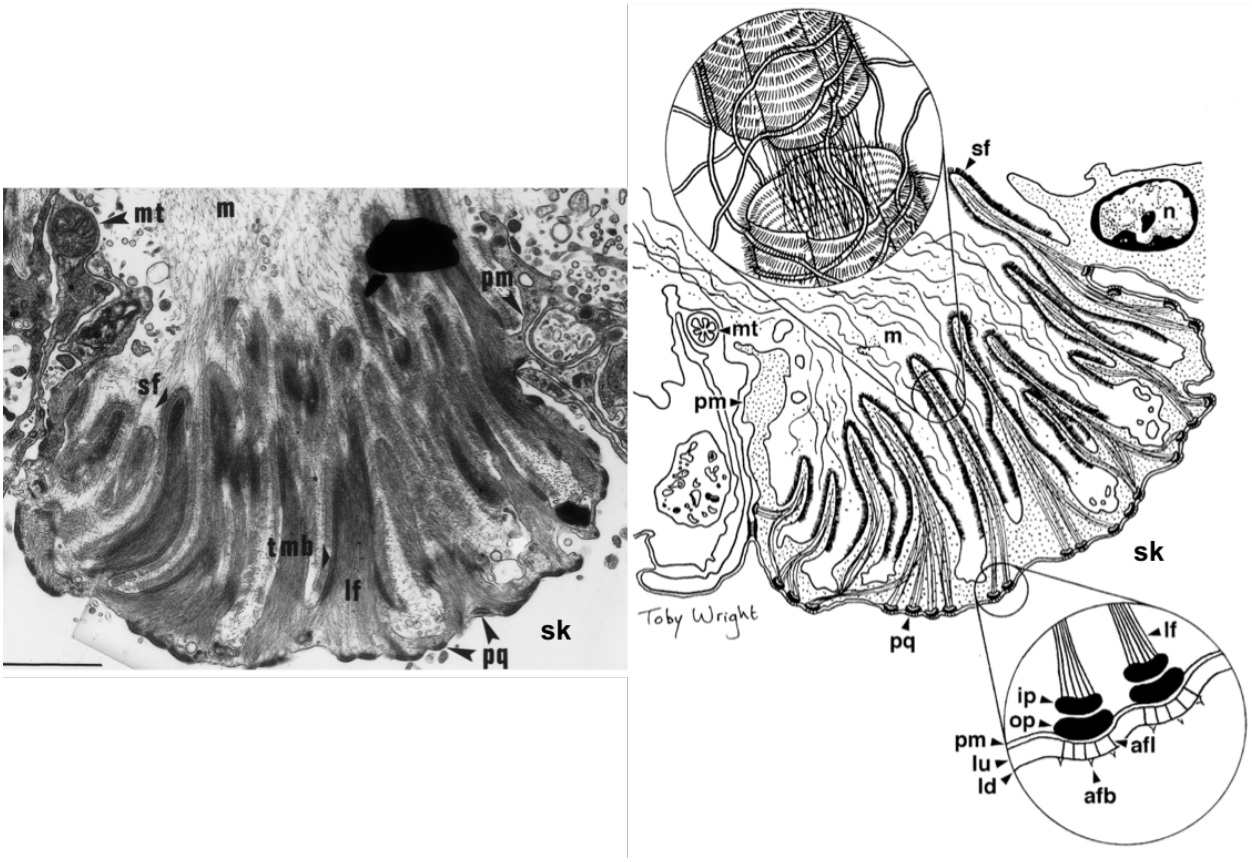

Figure 12. From Muscatine et al. 1997. Transmission electron micrograph and illustration of a desmocyte in *S. pistillata* showing desmocyte tenons interdigitating with mesoglea mortises, general arrangement of the short and long fibers of the tenons, invaginations of the plasma membrane, and the distal plaques at the skeleton interface. Scale bar is 1 μm. Illustration not drawn to scale. afb: anchoring fibrils, afl: anchoring filaments, cm: calicoblastic membrane, co: coelenteron, d: desmocyte, ip: inner plaque, lf: longitudinal fibers, ld: lamina densa, lu, lamina lucida, m: mesoglea, mt: mitochondrion, n: nucleus, op: outer plaque, pm: plasma membrane, pq: plaques, sf: short fibers, sk: skeleton, tmb: tenon boundary membrane.

ayRh localizes to symbiosome membrane of gastrodermal cells

The anti-ayRh antibody consistently labeled structures inside coral gastrodermal cells in tissue sections of decalcified branches (Fig. 11C). However, identifying the precise subcellular localization of ayRh was impossible due to the high density and compact organization of gastrodermal cells. To get a clearer view of ayRh's localization in gastrodermal cells, cells were isolated and fixed for immunocytochemistry. Controls were repeated for isolated cells again showing specificity of the anti-ayRh antibody for immunofluorescence microscopy (Fig. 13). Limited algal autofluorescence in the red

channel remained visible in control images, but it was significantly dimmer compared to ayRh immunofluorescence.

An initial characterization of cell isolates from daylight hours confirmed ayRh was localized to *Symbiodinium*-hosting gastrodermal cells, and specifically surrounding *Symbiodinium*, but never surrounding the nucleus of the host coral cell (Fig. 13A). This staining pattern is indicative of ayRh localization in the host cell cytoplasm or in the symbiosome membrane, but not in the plasma membrane of the coral host cell (Barott et al. 2015a).

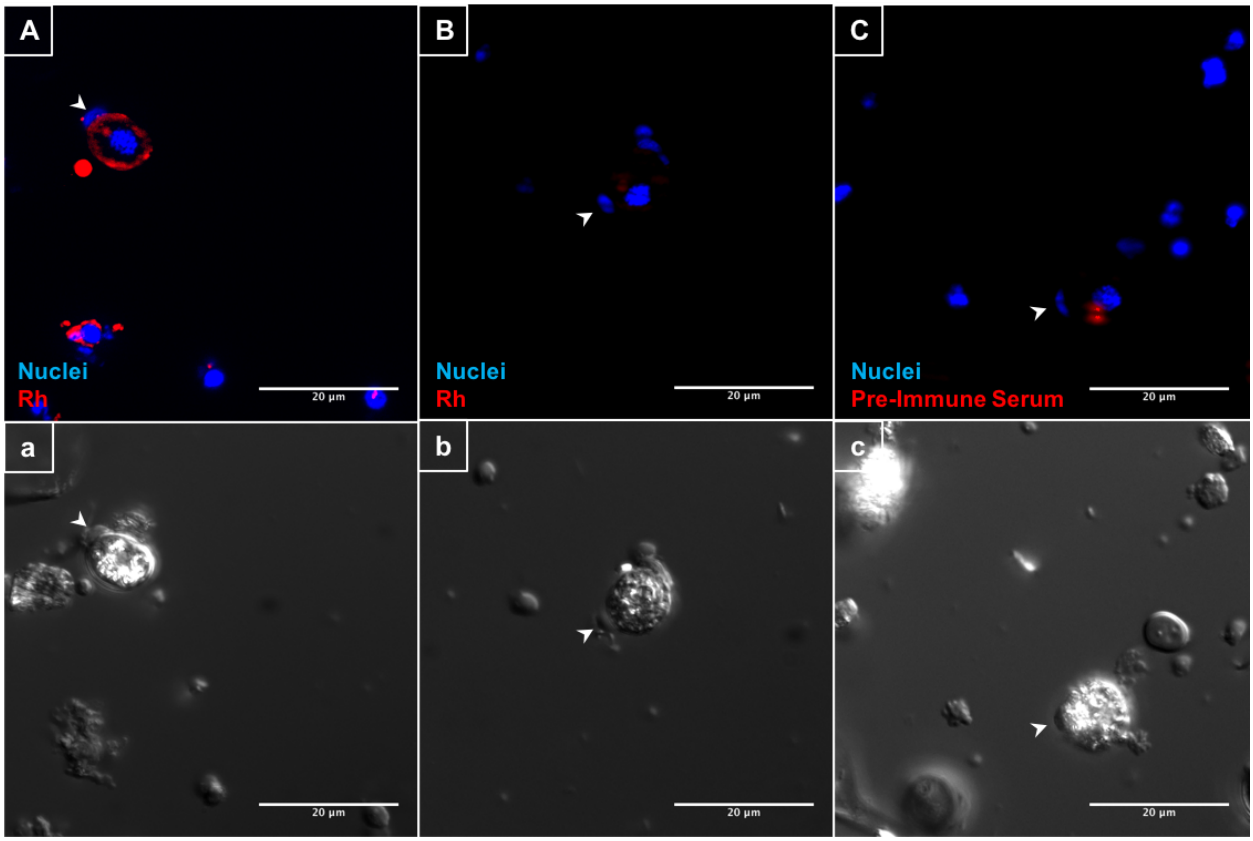

Figure 13. Rh immunofluorescence microscopy controls of isolated *A. yongei* gastrodermal cells. (A) Anti-Rh antibody only, (B) peptide pre-absorption control, and (C) rabbit pre-immune serum control. Staining of the symbiosome membrane is displayed in panel A. Nuclei are labeled in blue and Rh in red. Panels A-C show nuclear and Rh staining while panels a-c show accompanying DIC images to illustrate cell structure. Controls show reduction of red channel signal confirming antibody optimization. Algal autofluorescence in the red channel remains visible. Native GFP signal is not shown. White arrowheads show the small nuclei of the coral host; larger, speckled nuclei belong to hosted *Symbiodinium*.

ayRh and VHA signal show differing patters during dark and light conditions

Following confirmation of ayRh localization to gastrodermal cells, exploratory branch clippings were taken at 03:00 (dark) and 08:30 (light) and immunolabeled for VHA and ayRh. While VHA in gastrodermal cells seemed homogeneous in terms of signal intensity and subcellular between sections from 03:00 and 08:30 (Fig. 14), ayRh pattern was heterogeneous: sections from 03:00 appeared to display lower and more diffuse signal in gastrodermal cells than those from 08:30 (Fig. 14).

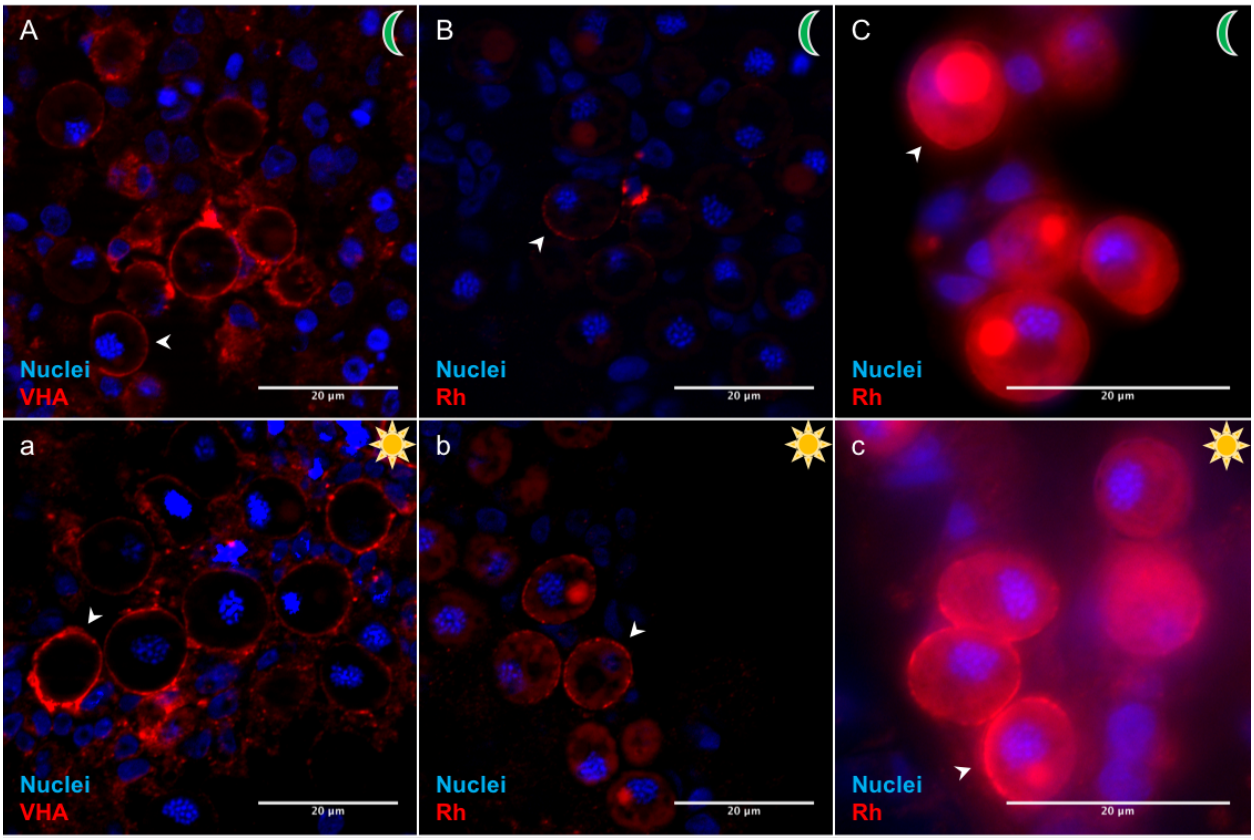

Figure 14. Comparison of Rh and VHA localization by immunofluorescence microscopy in *A. yongei* branches during dark and light conditions. (A-a) VHA in dark and light conditions showing no apparent change in gastrodermal cell localization. (B-b, C-c) Rh in dark and light conditions at low and high magnification. Rh signal intensity is variable and labeling appears more diffuse in dark conditions. Moons indicate dark conditions while suns indicate light conditions. Nuclei are labeled in blue. VHA and Rh are labeled in red accordingly. Red algal autofluorescence is especially visible in panels b, C, and c.

ayRh appears to traffic to the symbiosome membrane on a diel cycle

To investigate the heterogeneous ayRh subcellular localization further, cell isolations were performed at 6 time points along a diel cycle and immunostained for ayRh. There were significant changes in the proportion of cells showing ayRh localization in the symbiosome membrane and host cell cytoplasm, with the largest proportion of cells exhibiting symbiosome localization at 13:00 (52%; N=3) and the lowest at 23:00 (31%; N=3) ($p=0.0246$). ayRh appeared to traffic away from the symbiosome membrane to the host cytoplasm as dusk and midnight approached (13:00-23:00), and to be inserted back into the symbiosome membrane approaching dawn and midday (23:00-08:30) (Fig. 15). Results of individual trials are reported in the appendix (Fig. 18).

Figure 15. Diel trends in Rh localization in *Symbiodinium*-hosting coral gastrodermal cells. Rh appears to traffic from the symbiosome membrane to the cytoplasm of the host cell in isolated *A. yongei* cells. (A) Rh signal location in gastrodermal cells as a function of time (N=3). (B) Percent of cells with Rh signal on the symbiosome membrane as a function of time; data transformed by y=arcsin(sqrt(x)) as per Wang & Douglas 1998, Barott et al. 2013. Shaded regions denote dark conditions (18:00-08:00). Error bars represent standard deviation. Statistically significant differences are denoted by * (Friedman Test, $p<0.005$).

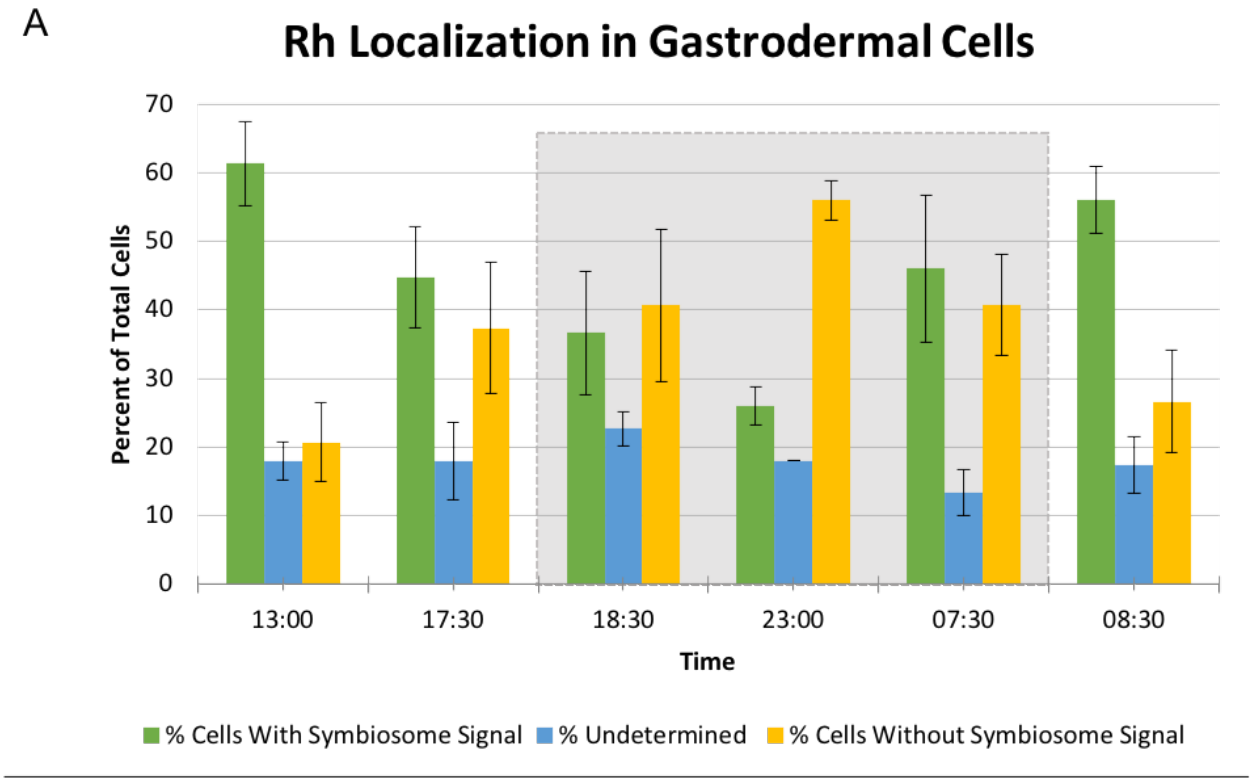

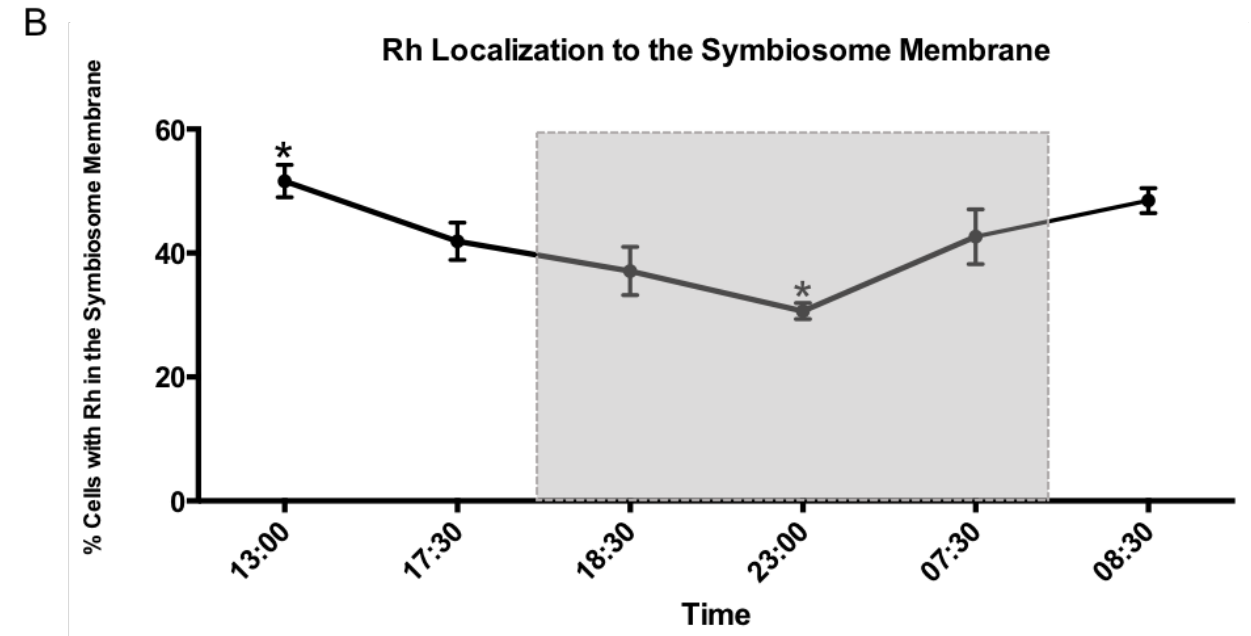

VHA may traffic to the symbiosome membrane on a diel cycle

Additionally, two of those cell isolations from 13:00 and a 23:00 were immunostained for VHA. The analysis is only qualitative because of the lack of replication (N=1). Many coral cells exhibited symbiosome staining during both day and night but VHA signal appeared patchier and harder to classify; this pattern was less prominent in the sample from 23:00 (Fig. 16).

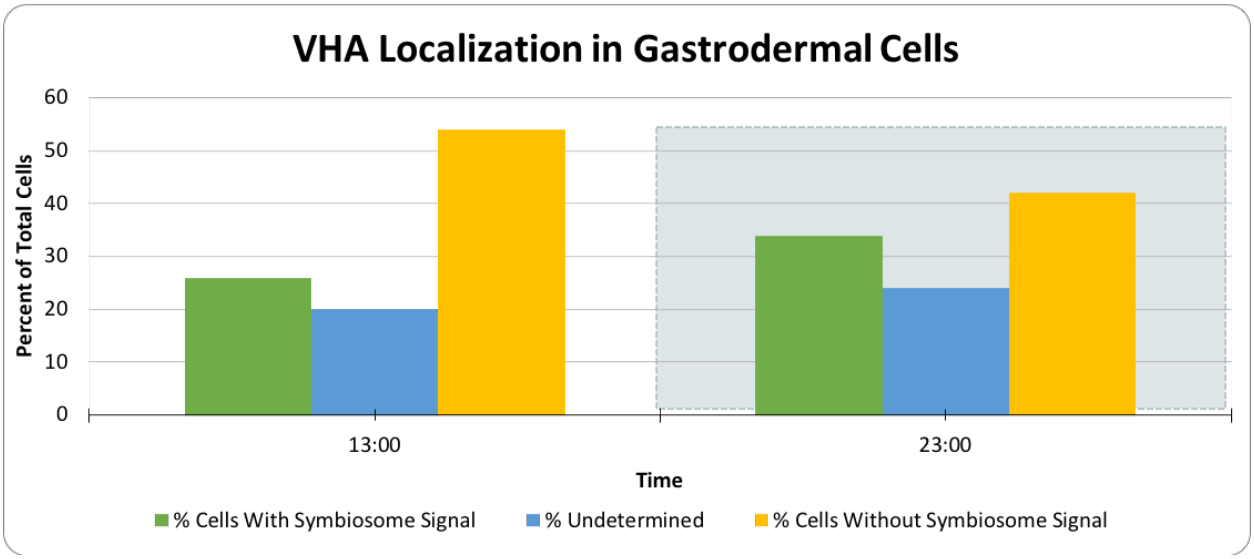

Figure 16. Diel trend in VHA localization in *Symbiodinium*-hosting coral gastrodermal cells. VHA may traffic from the cytoplasm to the symbiosome membrane of isolated *A. yongei* host cells (N=1). Shaded regions denote dark conditions (18:00-08:00).

DISCUSSION

ayRh seems to be a NH_3 gas channel

Here I present the first known characterization of a functional Rh protein in Cnidarians. Phylogenetic analysis grouped ayRh within the Rh family of proteins, specifically in the Rhp1 subgroup common to invertebrates (Fig. 7). ayRh is grouped alongside other Cnidarian Rh proteins suggesting functional conservation amongst this cohort. Notably, Rh genes from the green alga *Chlamydomonas reinhardtii* also group with Cnidarians in the Rhp1 cluster. Multiple studies have provided evidence for *C. reinhardtii* Rh being capable of transporting CO_2 in addition to NH_3 (Soupene et al. 2002, Soupene et al. 2004); sequence conservation between *C. reinhardtii* and *A. yongei* likewise suggests that ayRh may be capable of CO_2 transport.

The organization of this cladogram is largely in agreement with previous analysis (Huang & Peng 2005) with only minor deviation regarding the divergence of the Rh30 and organization of the Rhp1 subgroups. Regardless, the placement and organization of the Rh30 and Rhp1 subgroups were not well supported here nor in the original paper and do not impact the interpretation of this research nor the function of the Rhp1 subgroup as NH_3 gas channels.

Additional analysis further supports the phylogeny obtained in this thesis placing ayRh within the Rh protein family. Sequence analysis of the cloned ayRh gene predicted 12 transmembrane domains. This agrees with previous work showing Rh proteins have 12 unlike Meps and Amts that possess 11 (Marini et al. 2000, Benghezal et al. 2001). Consistent with studies on Rh proteins, sequencing and western blot analysis agreed that the ayRh gene encodes a ~52 kDa protein. This places ayRh in the

Rh50 group (including RhA-C and Rhps). These analyses strongly suggest that ayRh belongs to the larger Rh50 protein subfamily and as such is a putative NH_3 gas channel with potential CO_2 transporting capabilities.

While there is agreement that Rh proteins facilitate NH_3 movement across biological membranes it is still unclear whether they move existing NH_3 or if they help deprotonate NH_4^+ ions and then move NH_3. The hypothesis that many Rh proteins additionally facilitate CO_2 diffusion is also gaining strength. There is still considerable disagreement on the exact mechanisms behind Rh-mediated NH_3/CO_2 transport even in well-studied systems (Peng & Huang 2006, Weiner & Verlander 2017, Baday et al. 2015, Andrade & Einsle 2007, Khademi & Stroud 2006) so caution must be taken when addressing these issues in a poorly understood invertebrate group such as corals. For the remainder of this thesis I will make considerations to address these possible scenarios and address the physiologically relevant implications of NH_3 and CO_2 conductance.

Rh is present in the symbiosome membrane of A. yongei, constituting a diel NCM

This study localized ayRh to the symbiosome membrane of coral gastrodermal cells suggesting it plays a role in coral-*Symbiodinium* interactions. Furthermore, ayRh seems to translocate between the symbiosome membrane and the cytoplasm of coral gastrodermal cells following a diel trend. I hypothesize that ayRh's in the symbiosome membrane facilitates a coral-mediated NCM that increases available nitrogen for algal cellular processes such as the continual production of photosystem proteins during daylight hours.

Cell isolations revealed that ayRh may localize to the symbiosome membrane suggesting that it plays a role in regulating the amount of NH_3/NH_4^+ available to *Symbiodinium*. As a NH_3 gas channel, ayRh would enhance NH_3 diffusion into the acidic symbiosome space following the partial pressure gradient. Once inside the symbiosome the acidic pH (pH 4) would protonate NH_3 resulting in NH_4^+ trapping. While nearly all NH_3/NH_4^+ at the pH of the host's cytoplasm (pH 7.4) already exists as membrane-impermeable NH_4^+, Rh proteins in the human kidney can enhance NH_3 diffusion at even smaller pH gradients (7.1-5.5) (Gruswitz et al. 2010). In addition, some vertebrate Rh proteins are suggested to deprotonate NH_4^+ to generate and conduct NH_3 (reviewed in Andrade & Einsle 2007 and Khademi & Stroud 2006). If ayRh has the same ability, NH_3/NH_4^+ flux into the symbiosome would be further enhanced by movement of stripped H^+ by VHA. Uptake of NH_4^+ by *Symbiodinium* would further accelerate NH_3 diffusion from the host cell cytoplasm into the symbiosome space following mass of law action.

Another exciting finding was that ayRh subcellular localization was dynamic during a diel cycle: ayRh appears to traffic from the symbiosome membrane to the cytoplasm of host cells approaching 23:00 and return to the membrane approaching 13:00. The observed change in the proportion of cells with Rh localization in the symbiosome membrane was gradual with significant differences only between 13:00 and 23:00. This implies that ayRh trafficking may be a slow process with cell-specific rate variability. To my knowledge, this is the first report of a protein trafficking to and away from a cellular membrane in corals.

An alternative explanation for the observed pattern is that ayRh on the symbiosome membrane is continually degraded during daylight hours. The host cell

must then synthesize and traffic new ayRh to the symbiosome membrane. This would manifest as an overall decrease in the proportion of cells with ayRh on the symbiosome membrane approaching sunset, an increase approaching sunrise, and a constant proportion of cells exhibiting potential cytoplasmic trafficking and synthesis (% undetermined). We found no difference in the proportion of cells exhibiting undetermined ayRh localization over 24 hours ($p=0.1099$) consistent with a hypothesis of continual ayRh synthesis to compensate for degradation. The process by which daytime ayRh degradation would occur remains unknown however.

Regardless of the mechanism, intracellular *Symbiodinium* may experience a decreased supply of NH_3/NH_4^+ at night resulting from a lower abundance of ayRh on the symbiosome membrane. NH_3 diffusion across the symbiosome membrane my still occur even in the absence of ayRh as symbiosome pH has been shown to remain constant during dark periods thereby maintaining the pH gradient (Barott et al. 2015a). However, the rate of NH_3 diffusion into the symbiosome would be lower than that achieved by a NH_3 gas channel such as ayRh. Additionally, it is possible that modifications have been made to the symbiosome membrane to prevent NH_3 and CO_2 gas diffusion in the absence of ayRh; this could be achieved by altered lipid composition and decreased membrane fluidity as first postulated by Kikeri et al. 1989 and demonstrated by Lande et al. 1995.

Diel variations in ayRh localization could be explained as a mechanism to control the supply of NH_4^+ available to intracellular *Symbiodinium*. While the coral animal must supply *Symbiodinium* with nutrients for cellular maintenance and the production of photosynthetic products (amino acids, glycoproteins, sugars, etc.), delivery of excess

NH_4^+ could result in *Symbiodinium* overgrowth and mitosis (Davy et al. 2012, Wang & Douglas 1999). This can lead to the breakdown of the symbiosis, expulsion of the symbiont, and even host-cell death (Davy et al. 2012) so the coral animal must maintain strict control over the symbiosome space.

A coral-mediated supply of NH_3/NH_4^+ during daylight hours may provide *Symbiodinium* with a source of nitrogen only when required for the maintenance of photosystems and the production of photosynthesis-associated products. The 32 kDa reaction center of photosystem II must be continually replaced during photosynthesis as oxygen evolution irreparably damages cellular machinery (Greenberg et al. 1989, Anderson & Barber 1996). The decreased percentage of cells showing localization of ayRh in the symbiosome membrane approaching midnight may be a response to a slowed release of photosynthetic products and cession of photodamage. At this point, providing NH_3/NH_4^+ to *Symbiodinium* in excess of photosystem and general protein synthesis requirements would no longer benefit the coral animal and could prove detrimental. The return of ayRh to the symbiosome membrane as midday approached could likewise be seen as a preparatory step to boost NH_4^+ available to intracellular *Symbiodinium* thereby maximizing the overall output of end products generated during daylight hours.

With the proposed diel NCM in mind, we can reinterpret the findings of Grover et al. 2002, Pernice et al. 2012, and Wang & Douglas 1998 as showing coral control over nitrogen delivery to *Symbiodinium*. *S. pistillata*-hosted *Symbiodinium* are not under strict nitrogen limitation during daylight hours (Grover et al. 2002) indicating that NCMs may enhance daytime delivery in corals of the Robust clade; their potential diel nature

remains unexplored. Further evidence for the use of a NCM is provided by Pernice et al. 2012 who showed that intracellular *Symbiodinium* can fix NH_4^+ 14-23x more rapidly than their coral hosts. It would thus make evolutionary sense if corals evolved a mechanism to decrease the availability of NH_4^+ during non-photosynthetic hours. Additionally, *Aiptasia pulchella*, a model system for corals, displayed elevated NH_4^+ when *Symbiodinium*-depleted indicating animal control over nitrogen movement (Wang & Douglas 1998).

An ayRh-VHA complex may traffic from the symbiosome membrane in coral gastrodermal cells

Like previous work (Barott et al. 2015a), VHA was present in the symbiosome membrane. A novel result from this thesis however is that many cells possessed VHA localized to the cytoplasm and not the symbiosome membrane, suggesting VHA may also translocate between those two subcellular localizations. Data from cell isolations at 13:00 and 23:00 also indicate that like ayRh, VHA may in fact traffic to and from this membrane. It must be acknowledged however that only one sample from each time point was analyzed; this was due to time constraints associated with sample processing. Therefore, a potential VHA diel trafficking cannot be concluded. Additionally, and in accordance with previous work, VHA signal in isolated cells appears patchy and can be difficult to detect even at high magnification (Barott et al. 2015a, personal observations) making classification of VHA localization difficult. However, isolated gastrodermal cells still exhibited low symbiosome pH in both dark and light conditions (Barott et al. 2015a), suggesting that (1) some VHA always remain on the symbiosome membrane but cannot always be visualized or (2) the symbiosome can

remain highly acidic during these experiments (~10 minutes), despite lower VHA presence in the symbiosome membrane. The latter option implies that the protonation rate of molecules in the symbiosome is not constant over a diel cycle, as soaking of protons would raise pH and require additional VHA activity to secrete H^+; additionally, existing VHAs could upregulate H^+ secretion to compensate for lower VHA presence. The experiments of Barott et al. were carried out over much shorter time periods than this study however and their results may not be directly comparable with the findings of this thesis.

If VHA does indeed traffic from the symbiosome membrane, this opens the possibility of translocation in a complex with ayRh on a diel cycle. Previous work has shown that VHA and RhC form a complex on the apical membrane of human kidney cells (Bourgeois et al. 2017). Complexing with RhC was shown to stimulate H^+ secretion by VHA, resulting in increased NH_3/NH_4^+ excretion across the apical membrane and into urine; no reciprocal effect was found between VHA activity on RhC activity. RhB in human kidney cells has also been shown to modulate ion exchanger activity (Genetet et al. 2015). If the same mechanism extends to *A. yongei,* ayRh may stimulate VHA activity during daylight hours to maximize NH_3/NH_4^+ delivery into the symbiosome (Fig. 17). NH_3 transport and trapping as NH_4^+ would alkalinize the symbiosome requiring constant, higher VHA activity to maintain the H^+ gradient. While symbiosome pH remains acidic in the dark, reduced ayRh-NH_3 transport may imply less VHA activity is needed to maintain reduced pH. Future work should focus on expanding the sample size of VHA cell isolations and to observe the activity of VHA on a diel cycle.

It must also be noted that the cell isolations performed in this study report the proportion of cells with VHA in the symbiosome at much lower levels (25-32%) than in Barott et al. 2015a (86%). While this result could be interpreted as evidence of cell isolations altering the subcellular location of VHA, several caveats do exist. First, while branch images consistently show VHA signal in gastrodermal cells in day and night, they cannot be used to determine subcellular protein localization. As such, VHA may not always be embedded in the symbiosome membrane but still present at high levels in cytoplasm. This is consistent with the regulatory mechanisms for VHA activity including sequestration to cytoplasmic vesicles and subunit separation (Nanda et al. 1996, Sumner et al. 1995). Second, only one cell isolation sample was taken at each time point. Additional replicates are needed before any definitive conclusions can be made.

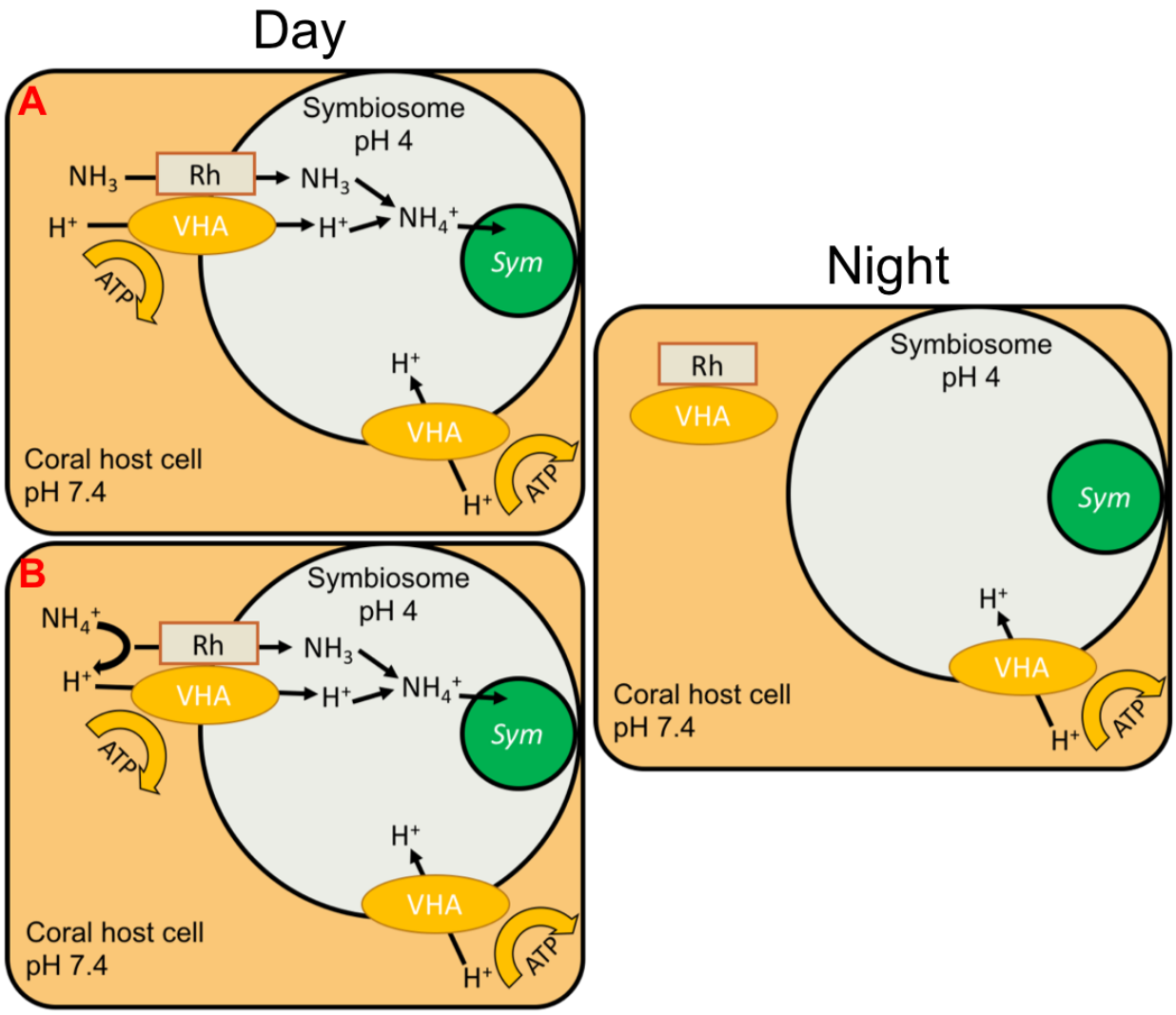

Figure 17. Model of the diel nitrogen concentrating mechanism (NCM) in *A. yongei*. A proposed Rh-VHA complex enhances NH_3/NH_4^+ delivery to intracellular *Symbiodinium* (Sym) during daylight hours and traffics to the coral host cell's cytoplasm at night. Scenarios for both (A) 'raw' NH_3 transport and (B) deprotonation of NH_4^+ by ayRh and accompanying VHA-H^+ transport are shown. Additional non-complexed VHA likely remains on the symbiosome membrane permanently to maintain low symbiosome pH. ATP: Adenosine triphosphate, Rh: Rhesus protein (NH_3 gas channel), VHA: Vacuolar-type Proton-ATPase.

An ayRh-mediated NCM could also conduct CO_2 constituting a 'leaky' CCM

While the discussion above assumed ayRh is a NH_3 gas channel, ayRh may facilitate the diffusion of CO_2 in addition or instead of NH_3. However, if ayRh can facilitate CO_2 along partial pressure gradients, it could undermine the CCM for photosynthesis (Barott et al. 2015a) by mediating a backflow of CO_2 into the host cell's

cytoplasm. Exploring this possibility requires establishing ayRh permeability coefficient for NH_3 and CO_2. Even if ayRh allows backflow into the host's cytoplasm this rate may be outpaced by CO_2 input into the symbiosome space, and still be a CCM with additional NH_4^+ concentrating capabilities. This would represent a tradeoff between CO_2 concentrating efficiency and the need to deliver NH_4^+ to *Symbiodinium*.

Another potential interpretation of the interplay between *A. yongei's* CCM and proposed NCM is that low symbiosome pH first evolved as a mechanism to deliver NH_3/NH_4^+instead of CO_2, to *Symbiodinium*. At the evolutionary origins of symbiosis, *Symbiodinium* would still receive CO_2 via uptake-driven diffusion into the symbiosome space without a concentration mechanism. NH_3 diffusion would be much slower however as NH_4^+ is membrane-impermeable and the dominant species relevant pHs. Concentration mechanisms would therefore be necessary to alleviate the nitrogen starvation free-living *Symbiodinium* experience in the water column (Cook et al. 1994). The CCM would then have evolved within the existing framework of an ayRh-enhanced NCM; slight CO_2 backflow would thus be a necessary concession in order to provide essential NH_3/NH_4^+.

ayRh plays a role in desmocyte function and potentially in SCM pH regulation

In Fig. 10A, Fig. 11D, and Fig. 12 I presented evidence for ayRh localizing to the tenon boundary and apical membranes of *A. yongei* desmocytes. This is the first study to localize a protein to coral desmocytes; previous studies have provided morphological descriptions of this cell type implicating it in skeletal attachment but have not described any mechanisms associated with their function (Tidball 1982, Muscatine et al. 1997, Goldberg 2001b, Tambutté et al. 2007).

I propose that ayRh aids in the exchange of NH_3/NH_4^+ between the aboral mesoglea, desmocyte cytoplasm, and the SCM. Under SEM observations, desmocyte cytoplasm is notably filled by intracellular tenons of unknown proteinaceous composition, although both collagen and actin have been proposed (Muscatine et al. 1997). Formation, breakdown, and maintenance of these extensive tenon networks likely require continuous protein synthesis and exchange of nitrogenous material with the mesoglea. Because NH_3/NH_4^+ are already abundant in Anthozoan tissues (58 nmol/mg protein) (Wang & Douglas 1998), they appear as ideal nitrogen species for this mechanism.

ayRh may additionally facilitate the diffusion of NH_3 from the mesoglea and across the calicobalstic cells to the SCM to maintain high pH (~9). The formation of one mole of $CaCO_3$ from DIC and Ca^{2+} produces two moles of H^+ thereby lowering pH in presumed calcifying vesicles in calicoblastic cells. In order to facilitate $CaCO_3$ formation, H^+ must continuously be removed from vesicles and any remaining at the time of fusion with the SCM will be released thereby lowering SCM pH. H^+ could then be removed by in the SCM by a buffering reaction such as that of a weak base like NH_3. Interestingly, the pKa of NH_3/NH_4^+ is remarkably close to measured SCM pH (pKa = 9.24) suggesting that NH_3/NH_4^+ may play a larger role in maintaining SCM pH than the removal of incidental H^+. NH_4^+ produced by protonation may additionally enhance the stability and conformational folding of multiprotein complexes in the SCM. High concentrations of NH_4^+ salts are commonly used in laboratory protein precipitation protocols (Green & Hughes 1955) but lower concentrations may be able to induce these effects especially in large complexes (Wingfield 2016).

If ayRh transported CO_2, its presence in desmocytes could also play a role in DIC delivery to the SCM. Partial pressure gradients would favor diffusion of CO_2 from cytoplasm into the SCM (pH ~9) and immediate dissociation into H^+ and HCO_3^+ and CO_3^{2-} While desmocyte pH has not been directly measured, it is likely close to that of neighboring cells in the aboral ectoderm (pH 7.4, Venn et al. 2011). Desmocyte ayRh may thus enhance both the buffering capacity and DIC concentration of the SCM.

ayRh may facilitate NH_3/NH_4^+ transport excretion across the oral ectoderm

In addition to coral endodermal cells and desmocytes, ayRh was relatively highly present in the apical membrane of oral ectoderm cells. A similar localization pattern has been reported in NH_3/NH_4^+ excretory epithelia from mytilid mussels (Thomsen et al. 2016), and cephalopods (Hu et al. 2014). I propose that, in our aquarium setting, ayRh enhances NH_3 diffusion into seawater in a similar fashion to these marine invertebrate systems. It is not clear if this putative mechanism for NH_3 excretion involves acid trapping, as VHA does not seem to be present in the apical membrane of coral oral ectodermal cells, and NHEs have not been studied in corals yet. However, NH_3 diffusion could be enhanced by stirring of the surface boundary layer by coral microvilli in a mechanism similar to that of mussel gill and plicate organ (Thomsen et al. 2016). In mussel plicate organ, VHA abundance in the apical membrane was shown to increase when acclimated to artificially alkalinized seawater, presumably to counter NH_3 backflow into the cell. A similar response may be inducible in *A. yongei* and future work could address this possibility experimentally. ayRh may also play a role in pH_c regulation of oral ectodermal cells if it's capable of facilitating CO_2 diffusion. Partial pressure and pH gradients dictate CO_2 would diffuse from the cytoplasm of coral cells into seawater

thereby raising pH_c. Future work to establish the ayRh permeability coefficients of NH_3 and CO_2 will help clarify this protein's function on the oral ectoderm.

In non-aquarium settings, such as in a coral reef, ayRh on the apical membrane of the oral ectoderm may facilitate NH_3 diffusion into cell cytoplasm. Water for flow-through aquaria at Scripps Institution of Oceanography is sourced from the coastal Pacific Ocean where NH_3, NH_4^+, and general nutrient levels are much higher than oligotrophic reefs. In a pristine, nitrogen-limited coral reef, *A. yongei* would likely seek to conserve nitrogen. The mucus layer directly overlaying the oral ectoderm hosts an extensive microbiome of nitrogen-fixing bacteria (Lema et al. 2012) and partial pressure gradients would favor NH_3 diffusion into the coral colony via the ayRh pathway. *A. yongei* also abundantly express NKA along the apical membrane of the oral ectoderm (Barott et al. 2015b) constituting a potential NH_4^+ uptake pathway. Future work can address this discrepancy by raising corals in seawater with varied nitrogen levels and observing changes in ayRh, NKA, VHA, and NHE localization patterns in the oral tissues.

Conclusions

This thesis indicates that ayRh is an NH_3 gas channel with the potential to additionally transport CO_2 in relation to a variety of physiological processes in multiple coral cell types. First, ayRh localization to the symbiosome membrane may constitute a novel Cnidarian NCM. Furthermore, Rh-dependent NH_3/NH_4^+ supply to *Symbiodinium* appears to vary on a diel cycle basis, possibly as a mechanism that allows coral host cells to regulate symbiont metabolism and growth. Preliminary evidence for potential trafficking of VHA from the symbiosome suggest the existence of an ayRh-VHA

complex, similar to human kidney cells, that traffics as a single unit. Future work should address this hypothesis.

Second, ayRh appears to play a role in calcification possibly by mediating the attachment of desmocyte to the skeleton or by affecting the chemical and physical properties of the SCM. Diffusion of NH_3 from desmocytes via Rh may play a role in SCM pH regulation or in integration with the aboral mesoglea. A dearth of knowledge exists regarding coral desmocyte functioning and additional mechanistic studies are required before any conclusions can be drawn.

Finally, ayRh appears to be involved in facilitating nitrogenous waste excretion across the apical membrane of oral ectodermal cells, possibly enhanced by microvilli movement akin to ciliary beating in mussels.

Additional research to understand the cellular mechanisms behind basic physiological processes in corals is critical to developing management regimes to protect species in the face of climate change. Mechanistic variance between species, clades, life stages, seasons, and stressors are all poorly understood, and resources should be devoted to basic research. Generating a clearer understanding of these systems should be a priority so future regulations and conservation strategies can more comprehensively address the threats facing coral health. Understanding the *whys* behind coral mortality and stress will provide a basis for altered human activity to safeguard these valuable ecosystems. My thesis can help achieve these goals by providing a framework to begin to understand the dynamic physiological mechanisms relating seawater nitrogen content, coral holobiont biology, the coral-*Symbiodinium* relationship, and whole-reef ecology. Future research should incorporate these findings

when addressing eutrophication on reefs, coral bleaching events, changing ocean chemistry, and ocean warming. Eutrophication of coral reefs and warming ocean temperatures may undermine the ability of corals to regulate nitrogen delivery to *Symbiodinium* thereby releasing them from coral control. Coupled with higher metabolic and enzyme reaction rates observed during elevated seawater temperatures, degradation of a coral controlled NCM may increase the risk of *Symbiodinium* expulsion, coral bleaching, and colony mortality.

Future research

This thesis has taken a definitive step in characterizing the ayRh protein and its role in coral physiology however, future work can add meaning to my findings: first, the permeability of ayRh to NH_3 and CO_2 gasses should be assessed. These results would eliminate ambiguity in my proposed models for *A. yongei* and provide insight into the larger role of proteins in the Rhp1 subgroup. This work is currently ongoing.

Second, the sample size for cell isolations should be expanded with additional trials. While three trials at six time points were conducted for ayRh cell isolations, only one trial at two time points was carried out for VHA. Additional sampling will clarify if VHA exhibits similar diel localization changes to ayRh.

Third, the hypothesis of an ayRh-VHA complex should be tested. This could be accomplished by testing if ayRh continues to traffic while VHA is under drug-inhibition. Another approach could manipulate seawater pH and [NH_3/NH_4^+] while observing the diel patterns of ayRh and VHA expression and localization.

Finally, the evolutionary relationship between the NCM and CCM can be investigated. Corals from the Robust clade should be examined for evidence of NCMs

utilizing Rh proteins. As both Complex and Robust clades possess mechanistically similar CCMs (Barott et al. 2015a), existence of Rh-associated NCMs in both would suggest a conserved role in symbiosis that evolved before the divergence event. A lack of Rh-involvement in Robust NCMs would indicate independent evolution of the NCM after clade divergence, akin to calcification mechanisms, and therefore a CCM-first evolutionary history.

Acknowledgments

This work contains material that is being prepared for publication: Thies A, Barron M, Tresguerres M. An Rh protein in coral constitutes a novel diel nitrogen concentrating mechanism to regulate *Symbiodinium* growth. *American Journal of Physiology – Cell Physiology*.

APENDIX

Figure 18. Results of individual cell isolation trials to identify the subcellular localization of Rh in *A. yongei* gastrodermal cells. Shaded regions denote dark conditions (18:00-08:00).

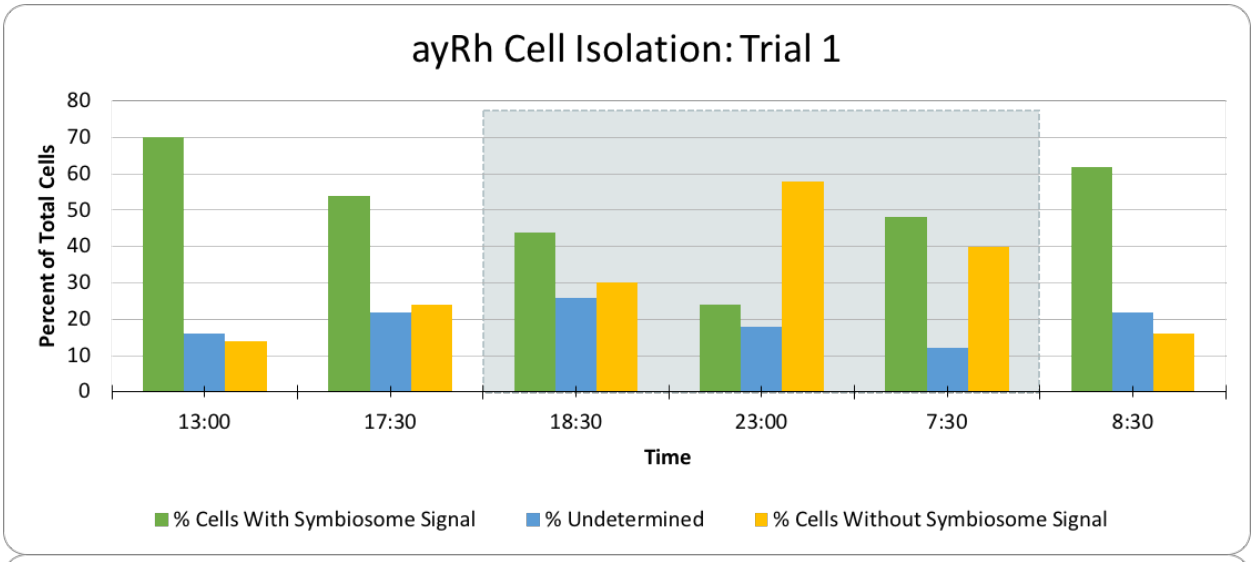

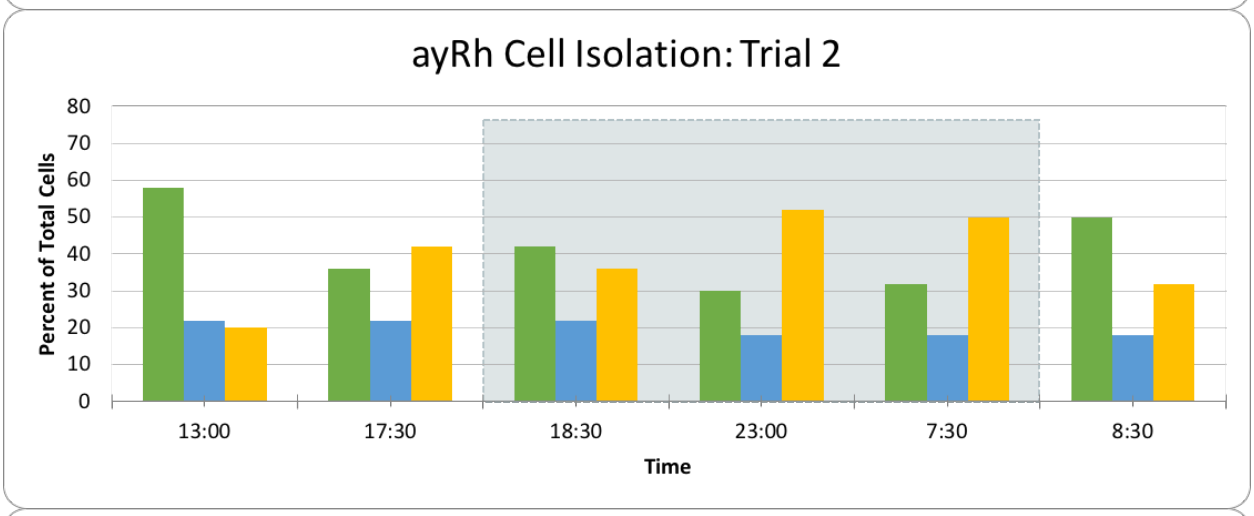

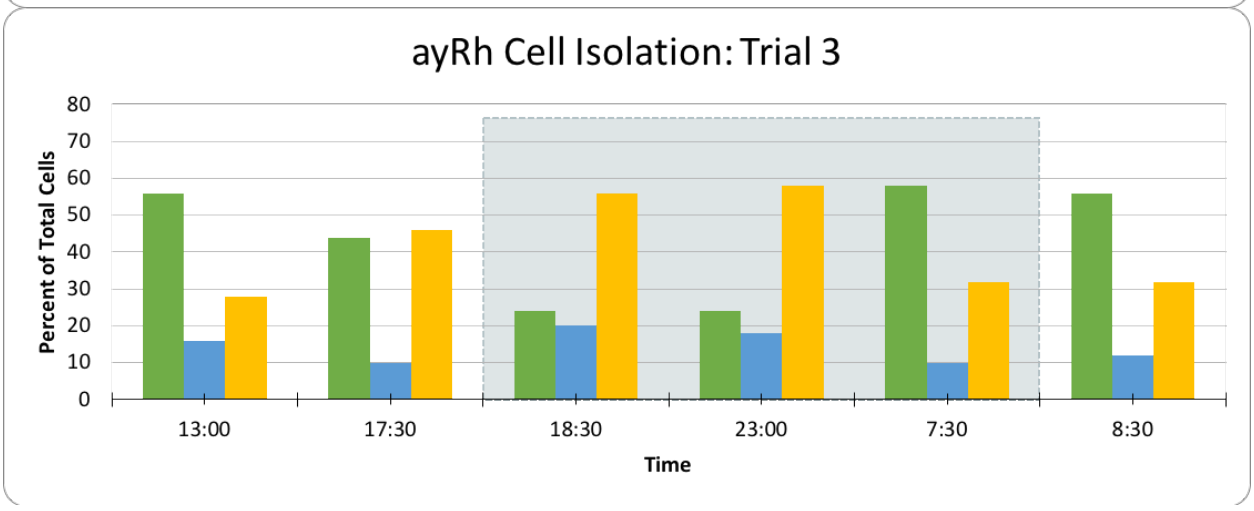

REFERENCES

1. **Agostini S, Suzuki Y, Higuchi T, Casareto BE, Yoshinaga K, Nakano Y, Fujimura H.** Biological and chemical characteristics of the coral gastric cavity. *Coral Reefs* 31: 147–156, 2011.

2. **Al-Horani FA**, **Al-Moghrabi SM**, **de Beer D**. The mechanism of calcification and its relation to photosynthesis and respiration in the scleractinian coral Galaxea fascicularis. *Mar Biol* 142: 419–426, 2003.

3. **Allemand D**, **Tambutté É**, **Zoccola D**, **Tambutté S**. Coral Calcification, Cells to Reefs. In: *Coral Reefs: An Ecosystem in Transition*, edited by Dubinsky Z, Stambler N. London, UK. Springer Dordrecht Heidelberg, 2011, p. 119–150.

4. **Allemand D**, **Furla P**, **Bénazet-Tambutté S**. Mechanisms of carbon acquisition for endosymbiont photosynthesis in Anthozoa. *Can J Bot* 76: 925–941, 1998.

5. **Andersson B, Barber J**. (1996) Mechanisms of Photodamage and Protein Degradation During Photoinhibition of Photosystem II. In: *Photosynthesis and the Environment. Advances in Photosynthesis and Respiration*, edited by Baker, NR. Springer Dordrecht, Germany, 1996.

6. **Andrade SLA**, **Einsle O**. The Amt/Mep/Rh family of ammonium transport proteins (Review). *Mol Membr Biol* 24: 357–365, 2007.

7. **Aronson RB**, **Macintyre IG**, **Precht WF**, **Murdoch TJT**, **Wapnick CM**. The expanding scale of species turnover events on coral reefs in Belize. *Ecol Monogr* 72: 233–249, 2002.

8. **Baday S**, **Orabi EA**, **Wang S**, **Lamoureux G**, **Bernèche S**. Mechanism of NH4+ Recruitment and NH3 Transport in Rh Proteins. *Structure* 23: 1550–1557, 2015.

9. **Barott KL**, **Barron ME**, **Tresguerres M**. Identification of a molecular pH sensor in coral. *Proc R Soc B* 284: 1–8, 2017.

10. **Barott KL**, **Venn AA**, **Perez SO**, **Tambutté S**, **Tresguerres M**. Coral host cells acidify symbiotic algal microenvironment to promote photosynthesis. *Proc Natl Acad Sci U S A* 112: 607–12, 2015a.

11. **Barott KL**, **Perez SO**, **Linsmayer LB**, **Tresguerres M**. Differential localization of ion transporters suggest distinct cellular mechanisms for calcification and photosynthesis between two coral species. *Am J Physiol Regul Integr Comp Physiol* 13: 170–184, 2015b.

12. **Barott KL**, **Helman Y**, **Haramaty L**, **Barron ME**, **Hess KC**, **Buck J**, **Levin LR**, **Tresguerres M**. High adenylyl cyclase activity and in vivo cAMP fluctuations in

corals suggest central physiological role. *Sci Rep* 3, 2013.

13. **Benghezal M, Gotthardt D, Cornillon S, Cosson P**. Localization of the Rh50-like protein to the contractile vacuole in Dictyostelium. *Immunogenetics* 52 :284–288, 2001.

14. **Bergeron MJ, Gagnon E, Wallendorff B, Lapointe JY, Isenring P**. Ammonium transport and pH regulation by K^+-Cl^- cotransporters. *AmJ Physiol Renal Physiol* 285: F68–F78, 2003.

15. **Blanco G, Mercer RW**. Isozymes of the Na-K-ATPase: Heterogeneity in structure, diversity in function. *Am J Physiol* 275: F633–F650, 1998.

16. **Bourgeois S**, **Bounoure L**, **Mouro-Chanteloup I**, **Colin Y**, **Brown D**, **Wagner CA**. The ammonia transporter RhCG modulates urinary acidification by interacting with the vacuolar proton-ATPases in renal intercalated cells. *Kidney Int* 93: 390–402, 2017.

17. **Bourgeois S, Meer LV, Wootla B, Bloch-Faure M, Chambrey R, Shull GE, Gawenis LR, Houillier P**. NHE4 is critical for the renal handling of ammonia in rodents. *J Clin Invest* 120: 1895–1904, 2010.

18. **Carpenter K**, **Abrar M**, **Aeby G**, **Aronseon R**, **Banks S**, **Bruckner A**, **Chiriboga A**, **Cortés J**, **Delbeek JC**, **Devantier L**. Climate Change and Local Impacts. *Science* 321: 560–563, 2008.

19. **Carrisoza-Gaytán R**, **Rangel C**, **Salvador C**, **Saldaña-Meyer R**, **Escalona C**, **Satlin LM**, **Liu W**, **Zavilowitz B**, **Trujillo J**, **Bobadilla NA**, **Escobar LI**. The hyperpolarization-activated cyclic nucleotide-gated HCN2 channel transports ammonium in the distal nephron. *Kidney Int* 80: 832–840, 2011.

20. **Carté BK**. Potential of Marine Biomedical Natural Products research and medical applications. *Oxford Journals* 46: 271–286, 1996.

21. **Catala-Stucki R**. Fluorescent Effects from Corals irradiated with Ultra-Violet Rays. *Nature* 183: 949, 1959.

22. **Chambrey R**, **Goossens D**, **Bourgeois S**, **Picard N**, **Bloch-Faure M**, **Leviel F**, **Geoffroy V**, **Cambillau M**, **Colin Y**, **Paillard M**, **Houillier P**, **Cartron JP**, **Eladari D**. Genetic ablation of Rhbg in the mouse does not impair renal ammonium excretion. *Am J Physiol Renal Physiol* 289: F1281-90, 2005.

23. **Chimetto LA, Brocchi M, Thompson CC, Martins RCR, Ramos HR, Thompson FL**. Vibrios dominate as culturable nitrogen-fixing bacteria of the Brazilian coral Mussismilia hispida. *Syst. Appl. Microbiol.* 31: 312–319, 2008.

24. **Cidon S, Nelson N**. A Novel ATPase in the Chrommaffin Granule Membrane. *Journal of Biological Chemistry* 258: 2892-2898, 1983.

25. **Cook C**, **Muller-Parker G**, **Orlandini CD**. Ammonium enhancement of dark carbon fixation and nitrogen limitation in zooxanthellae symbiotic with the reef corals Madracis mirabilis and Montastrea annularis. *Mar Biol* 118: 157–165, 1994.

26. **Copper P**. Ancient reef ecosystem expansion and collapse. *Coral Reefs* 13: 3–11, 1994.

27. **Cunning R, Silverstein RN, Baker AC**. Investigating the causes and consequences of symbiont shuffling in a multi-partner reef coral symbiosis under environmental change. *Proc. Biol. Sci.* 282: 20141725, 2015a.

28. **Cunning R, Vaughan N, Gillette P, Capo TR, Matté JL, Baker AC**. Dynamic regulation of partner abundance mediates response of reef coral symbioses to environmental change. *Ecology* 96: 1411–1420, 2015b.

29. **Davy SK**, **Allemand D**, **Weis VM**. Cell Biology of Cnidarian-Dinoflagellate Symbiosis. *Microbiol Mol Biol Rev* 76: 229–261, 2012.

30. **D'Elia C**, **Domotor S**, **Webb K**. Nutrient uptake kinetics of freshly isolated zooxanthellae*. *Mar Biol* 167: 157–167, 1983.

31. **Dereeper A**, **Guignon V**, **Blanc G**, **Audic S**, **Buffet S**, **Chevenet F**, **Guindon S**, **Lefort V**, **Lescot M**, **Gascuel O**. Phylogeny .fr: robust phylogenetic analysis for the non-specialist. *Nucleic Acids Res* 36: 465–469, 2008.

32. **Downs CA**, **Woodley CM**, **Richmond RH**, **Lanning LL**, **Owen R**. Shifting the paradigm of coral-reef "health" assessment. *Mar Pollut Bull* 51: 486–494, 2005.

33. **Drake JL**. The Skeletal Proteome and Production of Calcifying Proteins in the Stony Coral Stylophora Pistillata. The State University of New Jersey, Rutgers: 2015.

34. **Drake JL**, **Mass T**, **Haramaty L**, **Zelzion E**, **Bhattacharya D**, **Falkowski PG**. Proteomic analysis of skeletal organic matrix from the stony coral Stylophora pistillata. *Proc Natl Acad Sci* 110: 3788–3793, 2013.

35. **Endeward V, Cartron JP, Ripoche P, Gros G**. RhAG protein of the Rhesus complex is a CO2 channel in the human red cell membrane. *FASEB J* 22: 64–73, 2008.

36. **Fabiny JM, Jayakumar A, Chinault AC, Barnes EM**. Sequencing of the structural gene of the ammonium (methylammonium) transporter of *Escherichia coli*. *Fed Amer Soc Exp Bio J* 4: A1962

37. **Fantazzini P**, **Mengoli S**, **Pasquini L**, **Bortolotti V**, **Brizi L**, **Mariani M**, **Di Giosia M**, **Fermani S**, **Capaccioni B**, **Caroselli E**, **Prada F**, **Zaccanti F**, **Levy O**, **Dubinsky Z**, **Kaandorp JA**, **Konglerd P**, **Hammel JU**, **Dauphin Y**, **Cuif JP**, **Weaver JC**, **Fabricius KE**, **Wagermaier W**, **Fratzl P**, **Falini G**, **Goffredo S**. Gains and losses of coral skeletal porosity changes with ocean acidification acclimation. *Nat Commun* 6: 7785, 2015.

38. **Fehsenfeld S, Weihrauch D**. Mechanisms of acid–base regulation in seawater-acclimated green crabs (Carcinus maenas). *Can J Zool* 94: 95–107, 2016a.

39. **Fehsenfeld S**, **Weihrauch D**. The role of an ancestral hyperpolarization-activated cyclic nucleotide-gated K+ channel in branchial acid-base regulation in the green crab, Carcinus maenas. *J Exp Biol* 219: 887–896, 2016b.

40. **Furla P**, **Galgani I**, **Durand I**, **Allemand D**. Sources and mechanisms of inorganic carbon transport for coral calcification and photosynthesis. *J Exp Biol* 203: 3445–3457, 2000.

41. **Furla P, Bénazet-Tambutté S, Jaubert J, Allemand D**. Functional polarity of the tentacle of the sea anemone Anemonia viridis: role in inorganic carbon acquisition. *Am. J. Physiol.* 274: R303–R310, 1998.

42. **Gates RD, Baghdasarian G, Muscatine L**. Temperature Stress Causes Host Cell Detachment in Symbiotic Cnidarians: Implications for Coral Bleaching. *Bio Bull* 182: 324-332, 1992.

43. **Genetet S, Ripoche P, Le Van Kim C, Colin Y, Lopez C**. Evidence of a structural and functional ammonium transporter RhBG.anion exchanger 1.ankyrin-G complex in kidney epithelial cells. *J Biol Chem* 290: 6925–6936, 2015.

44. **Gisselmann G**, **Marx T**, **Bobkov Y**, **Wetzel CH**, **Neuhaus EM**, **Ache BW**, **Hatt H**. Molecular and functional characterization of an I_h-channel from lobster olfactory receptor neurons. *Eur J Neurosci* 21: 1635–1647, 2005.

45. **Goldberg WM**. Feeding behavior, epidermal structure and mucus cytochemistry of the scleractinian Mycetophyllia reesi, a coral without tentacles. *Tissue and Cell* 34: 232–245, 2002a.

46. **Goldberg WM**. Gastrodermal structure and feeding responses in the scleractinian Mycetophyllia reesi, a coral with novel digestive filaments. *Tissue and Cell* 34: 246–261, 2002b.

47. **Goldberg WM**. Acid polysaccharides in the skeletal matrix and calicoblastic epithelium of the stony coral Mycetophyllia reesi. *Tissue and Cell* 33: 376–387, 2001a.

48. **Goldberg WM**. Desmocytes in the calicoblastic epithelium of the stony coral Mycetophyllia reesi and their attachment to the skeleton. *Tissue and Cell* 33: 388-394, 2001b.

49. **Green AA, Hughes WL**. Protein solubility on the basis of solubility in aqueous solutions of salts and organic solvents. *Methods Enzymol* 1: 67-90, 1955.

50. **Greenberg BM**, **Gaba V**, **Canaani O**, **Malkin S**, **Mattoo AK**, **Edelman M**. Separate photosensitizers mediate degradation of the 32-kDa photosystem II reaction center protein in the visible and UV spectral regions. *Proc Natl Acad Sci USA* 86: 6617–6620, 1989.

51. **Grover R**, **Maguer J-F**, **Reynaud-vaganay S**, **Ferrier-Pagès C**. Uptake of ammonium by the scleractinian coral Stylophora pistillata: Effect of feeding, light, and ammonium concentrations. *Limnol Oceanogr* 47: 782–790, 2002.

52. **Gruswitz F**, **Chaudhary S**, **Ho JD**, **Schlessinger A**, **Pezeshki B**, **Ho C-M**, **Sali A**, **Westhoff CM**, **Stroud RM**. Function of human Rh based on structure of RhCG at 2.1 A. *Proc Natl Acad Sci* 107: 9638–9643, 2010.

53. **Hu MY, Guh YJ, Stumpp M, Lee JR, Chen RD, Sung PH, Chen YC, Hwang PP, Tseng YC**. Branchial NH_4^+-dependent acid-base transport mechanisms and energy metabolism of squid (Sepioteuthis lessoniana) affected by seawater acidification. Front Zool 11: 55–72, 2014.

54. **Huang C-H**. Molecular origin and variability of the Rh gene family: an overview of evolution, genetics and function. *Haematologica* 2: 15512-15517, 2008.

55. **Huang C-H**, **Peng J**. Evolutionary conservation and diversification of Rh family genes and proteins. *Proc Natl Acad Sci* 102: 15512–15517, 2005.

56. **Huang C-H**, **Liu PZ**. New insights into the Rh superfamily of genes and proteins in erythroid cells and nonerythroid tissues. *Blood Cells, Mol Dis* 27: 90–101, 2001.

57. **Huang C-H**, **Liu PZ**, **Cheng JG**. Molecular biology and genetics of the Rh blood group system. *Semin Hematol* 37: 150–165, 2000.

58. **Hughes TP**, **Barnes ML**, **Bellwood DR**, **Cinner JE**, **Cumming GS**, **Jackson JBC**, **Kleypas J**, **Van De Leemput IA**, **Lough JM**, **Morrison TH**, **Palumbi SR**, **Van Nes EH**, **Scheffer M**. Coral reefs in the Anthropocene. *Nature* 546: 82–90, 2017.

59. **Hughes TP**, **Connell JH**. Multiple stressors on coral reefs: a long-term perspective. *Limnol Oceanogr* 44: 932–940, 1999.

60. **Johnston IS**. The ultrastructure of skeletogenesis in hermatypic corals. *Int. Rev. Cytol.* 67: 171–214, 1980.

61. **Jokiel PL**. The reef coral two compartment proton flux model: A new approach relating tissue-level physiological processes to gross corallum morphology. *J Exp Mar Bio Ecol* 409: 1–12, 2011.

62. **Kawaguti S**. Zooxanthellae in the Corals Are Intercellular Symbionts. *Proc Jpn Acad* 40: 545–548, 1964.

63. **Kawaguti S**. On the physiology of reef corals. II. The effect of light on color and form of reefs. *Palau Trop. Biol. Stat. Stud.* 2: 199–208, 1937.

64. **Khademi S**, **Stroud RM**. The Amt/MEP/Rh family: structure of AmtB and the mechanism of ammonia gas conduction. *Physiology (Bethesda)* 21: 419–29, 2006.

65. **Kikeri D**, **Sun a**, **Zeidel ML**, **Hebert SC**. Cell membranes impermeable to NH3. *Nature* 339: 478–480, 1989.

66. **Kinsella JL, Aronson PS**. Interaction of NH_4^+ and Li^+ with the renal microvillus membrane Na^+-H^+ exchanger. *Am J Physiol Cell Physiol* 241: C220–C226, 1981.

67. **Knowlton N**, **Brainard RE**, **Fisher R**, **Moews M**, **Plaisance L**, **Caley MJ**. Coral Reef Biodiversity. In: *Life in the World's Oceans: Diversity, Distribution, and Abundance*. Chichester, UK. Wiley-Blackwell, 2010, p. 65–78.

68. **Krediet CJ, Ritchie KB, Paul VJ, Teplitski M**. Coral-associated micro-organisms and their roles in promoting coral health and thwarting diseases. *Proc. Biol. Sci.* 280: 20122328–20122328, 2013.

69. **Krogh A**, **Larsson B**, **von Heijne G**, **Sonnhammer ELL**. Predicting Transmembrane Protein Topology with a Hidden Markov Model : Application to Complete Genomes. *J Mol Biol* 305: 567–580, 2001.

70. **Kühl M, Cohen Y, Dalsgaard T, Jorgensen BB, Revsbech NP**. Microenvironment and photosynthesis of zooxanthellae in scleractinian corals studied with microsensors for O2, pH and light. *Mar. Ecol. Prog. Ser.* 117: 159–172, 1995.

71. **Kustu S, Inwood W**. Biological gas channels for NH3 and CO2: evidence that Rh (Rhesus) proteins are CO2 channels. *Transfus Clin Biol* 13: 103–110, 2006.

72. **Lande MB, Donovan JM, Zeidel ML**. The relationship between membrane fluidity and permeabilities to water, solutes, ammonia, and protons. *J Gen Physiol* 106: 67–84, 1995.

73. **Lema KA, Willis BL, Bourne DG**. Corals Form Characteristic Associations with Symbiotic Nitrogen-Fixing Bacteria. *Appl Environ Microbiol* 78: 3136-3144, 2012.

74. **Lesser MP, Mazel CH, Gorbunov MY, Falkowski PG.** Discovery of Symbiotic Nitrogen-Fixing Cyanobacteria in Corals. *Science* 305: 1–5, 2014.

75. **Lirman D**, **Bowden-Kerby A**, **Schopmeyer S**, **Huntington B**, **Thyberg T**, **Gough M**, **Gough T**, **Gough R**, **Gough Y**. A window to the past: documenting the status of one of the last remaining "megapopulations" of the threatened staghorn coral Acropora cervicornis in the Dominican Republic. *Aquat Conserv Freshw Ecosyst* 20: 773–781, 2010.

76. **Marini AM, Andre B**. In vivo N-glycosylation of the mep2 high-affinity ammonium transporter of Saccharomyces cerevisiae reveals an extracytosolic N-terminus. *Mol Microbiol* 38: 552–564, 2000.

77. **Mass T**, **Giuffre AJ**, **Sun C-Y**, **Stifler CA**, **Frazier MJ**, **Neder M**, **Tamura N**, **Stan C V.**, **Marcus MA**, **Gilbert PUPA**. Amorphous calcium carbonate particles form coral skeletons. *Proc Natl Acad Sci* 114: 201707890, 2017.

78. **Mass T**, **Putnam HM**, **Drake JL**, **Zelzion E**, **Gates RD**, **Bhattacharya D**, **Falkowski PG**. Temporal and spatial expression patterns of biomineralization proteins during early development in the stony coral Pocillopora damicornis. *Proc R Soc London B Biol Sci* 283: 20160322, 2016.

79. **Mass, T., Drake, J. L., Haramaty, L., Kim, J. D., Zelzion, E., Bhattacharya, D. and Falkowski, P. G**. Cloning and characterization of four novel Coral Acid- Rich Proteins that precipitate carbonates *in vitro*. *Current Biology* 23: 1126–1131, 2013.

80. **Masui DC, Furriel RPM, Mantelatto FLM, McNamara JC, Leone FA**. K+ - phosphatase activity of gill (Na+, K+)-ATPase from the blue crab, Callinectes danae: low-salinity acclimation and expression of the alpha-subunit. J Exp Zool 303A: 294–307, 2005.

81. **Mitchinson C**, **Pain RH**. Effects of sulphate and urea on the stability and reversible unfolding of β-lactamase from Staphylococcus aureus. Implications for the folding pathway of β-lactamase. *J Mol Biol* 184: 331–342, 1985.

82. **Musa-Aziz R, Chen LM, Pelletier MF, Boron WF**. Relative CO2/NH3 selectivities of AQP1, AQP4, AQP5, AmtB, and RhAG. Proc Natl Acad Sci U S A 106:5406–5411, 2009.

83. **Muscatine L**, **Tambutté E**, **Allemand D**. Morphology of coral desmocytes, cells that anchor the calicoblastic epithelium to the skeleton. *Coral Reefs* 16: 205–213, 1997.

84. **Nanda A**, **Brumell JH**, **Nordström T**, **Kjeldsen L**, **Sengeløv H**, **Borregaard N**, **Rotstem OD**, **Grinstein S**. Activation of proton pumping in human neutrophils occurs by exocytosis of vesicles bearing vacuolar-type H+-ATPases. *J Biol Chem* 271: 15963–15970, 1996.

85. **Palmgren MG, Nissen P**. P-type ATPases. *Annu Rev Biophys* 40: 243–266, 2011.

86. **Peng J**, **Huang CH**. Rh proteins vs Amt proteins: an organismal and phylogenetic perspective on CO2 and NH3 gas channels. *Transfus Clin Biol* 13: 85–94, 2006.

87. **Pernice M**, **Meibom A**, **Van Den Heuvel A**, **Kopp C**, **Domart-Coulon I**, **Hoegh-Guldberg O**, **Dove S**. A single-cell view of ammonium assimilation in coral-dinoflagellate symbiosis. *Isme J* 6: 1314–1324, 2012.

88. **Perry SF, Braun MH, Noland M, Dawdy J, Walsh PJ**. Do zebrafish Rh proteins act as dual ammonia- CO2 channels? J Exp Zool A Ecol Genet Physiol 313: 618–621, 2010.

89. **Phillips JH**. Immune mechanisms in the phylum Coelenterata. In: *The Lower Metazoa*, edited by Dougherty EC. University of California Press, 1963, p. 425-431.

90. **Rädecker N**, **Pogoreutz C**, **Voolstra CR**, **Wiedenmann J**, **Wild C**. Nitrogen cycling in corals: The key to understanding holobiont functioning? *Trends Microbiol* 23: 490–497, 2015.

91. **Raina JB, Dinsdale EA, Willis BL, Bourne DG**. Do the organic sulfur compounds DMSP and DMS drive coral microbial associations? *Trends Microbiol.* 18: 101–108, 2010.

92. **Ramos-Silva P**, **Kaandorp J**, **Huisman L**, **Marie B**, **Zanella-Cléon I**, **Guichard N**, **Miller DJ**, **Marin F**. The skeletal proteome of the coral acropora millepora: The evolution of calcification by co-option and domain shuffling. *Mol Biol Evol* 30: 2099–2112, 2013.

93. **Rands M, Loughman B, Douglas A**. The symbiotic interface in an alga-invertebrate symbiosis. *Proc Biol Sci* 253:161–165, 1993.

94. **Rohwer F**, **Seguritan V**, **Azam F**, **Knowlton N**. Diversity and distribution of coral-associated bacteria. *Mar Ecol Prog Ser* 243: 1–10, 2002.

95. **Romano SL, Cairns SD**. Molecular phylogenetic hypotheses for the evolution of scleractinian corals. *Bulletin of Marine Science* 67: 1043–1068, 2000.

96. **Romano SL, Palumbi SR**. Evolution of Scleractinian Corals Inferred from Molecular Systematics. *Science* 271: 640–642, 1996.

97. **Sala E**, **Knowlton N**. Global Marine Biodiversity Trends. *Annu Rev Environ Resour* 31: 93–122, 2006.

98. **Seckbach J**. *Symbiosis: Mechanisms and Model Systems*. Kluwer Academic Publishers, 2002.

99. **Shinzato C**, **Shoguchi E**, **Kawashima T**, **Hamada M**, **Hisata K**, **Tanaka M**, **Fujie M**, **Fujiwara M**, **Koyanagi R**, **Ikuta T**, **Fujiyama A**, **Miller DJ**, **Satoh N**. Using the Acropora digitifera genome to understand coral responses to environmental change. *Nature* 476: 320–323, 2011.

100. **Sievers F**, **Wilm A**, **Dineen D**, **Gibson TJ**, **Karplus K**, **Li W**, **Lopez R**, **McWilliam H**, **Remmert M**, **Soding J**, **Thompson JD**, **Higgins DG**. Fast, scalable generation of high-quality protein multiple sequence alignments using Clustal Omega. *Mol Syst Biol* 7, 2011.

101. **Simon J**. Enzymology and bioenergetics of respiratory nitrite ammonification. FEMS Microbiol Rev 26: 285-309, 2002.

102. **Smith SV**. Coral-reef area and the contributions of reefs to processes and resources of the world's oceans Production of methane and carbon dioxide from methane thiol and dimethyl sulphide by anaerobic lake sediments. *Nature* 273: 225–226, 1978.

103. **Sonnhammer ELL**, **von Heijne G**, **Krogh A**. A hidden Markov model for predicting transmembrane helices in protein sequences. In: *Proceedings of the Sixth International Conference on Intelligent Systems for Molecular Biology*. 1998, p. 175–182.

104. **Soupene E, Inwood W, Kustu S**. Lack of the Rhesus protein Rh1 impairs growth of the green alga Chlamydomonas reinhardtii at high CO2. *Proc Natl Acad Sci USA* 101: 7787–92, 2004.

105. **Soupene E, King N, Feild E, Liu P, Niyogi KK, Huang CH, Kustu S**. Rhesus expression in a green alga is regulated by CO2. *Proc Natl Acad Sci USA* 99: 7769–73, 2002.

106. **Spalding MD**, **Grenfell AM**. New estimates of global and regional coral reef areas. *Coral Reefs* 16: 225–230, 1997.

107. **Stolarski J, Kitahara MV, Miller DJ, Cairns SD, Mazur M, Meibom A**. The ancient evolutionary origins of Scleractinia revealed by azooxanthellate corals. *BMC Evolutionary Biology* 11: 316, 2011.

108. **Sumner JP**, **Dow JAT**, **Earley FGP**, **Klein U**, **Jager D**, **Wieczorek H**. Regulation

of plasma membrane V-ATPase activity by dissociation of peripheral subunits. *J. Biol. Chem.* 270: 5649–5653, 1995.

109. **Tambutté E**, **Tambutté S**, **Segonds N**, **Zoccola D**, **Venn A**, **Erez J**, **Allemand D**. Calcein labelling and electrophysiology: insights on coral tissue permeability and calcification. *Proc R Soc B Biol Sci* 279: 19–27, 2011.

110. **Tambutté E**, **Allemand D**, **Zoccola D**, **Meibom A**, **Lotto S**, **Caminiti N**, **Tambutté S**. Observations of the tissue-skeleton interface in the scleractinian coral Stylophora pistillata. *Coral Reefs* 26: 517–529, 2007.

111. **Thomsen J**, **Himmerkus N**, **Holland N**, **Sartoris FJ**, **Bleich M**, **Tresguerres M**. Ammonia excretion in mytilid mussels is facilitated by ciliary beating. *J Exp Biol* 219: 2300–2310, 2016.

112. **Tidball JG**. Fine structural aspects of anthozoan desmocyte development (Phylum Cnidaria). *Tissue and Cell* 14: 85–96, 1982.

113. **Tresguerres M**, **Barott KL**, **Barron ME**, **Deheyn DD**, **Kline DI**, **Linsmayer LB**. Cell Biology of Reef-Building Corals: Ion Transport, Acid/Base Regulation, and Energy Metabolism. In: *Acid-Base Balance and Nitrogen Excretion in Invertebrates: Mechanisms and Strategies in Various Invertebrate Groups with Considerations of Challenges Caused by Ocean Acidification*, edited by Weihrauch D, O'Donnell M. Cham, Switzerland. Springer International Publishing, 2017, p. 193–218.

114. **Tresguerres M, Parks SK, Salazar E, Levin LR, Goss GG, Buck J**. Bicarbonate-sensing soluble adenylyl cyclase is an essential sensor for acid/base homeostasis. *Proc Natl Acad Sci USA* 107: 442–447, 2010.

115. **Tresguerres M, Katz S, Rouse GW**. How to get into bones: Proton pump and carbonic anhydrase in Osedax boneworms. *Proc Biol Sci* 280: 20130625, 2013.

116. **Udvardi M, Poole PS**. Transport and metabolism in legume-rhizobia symbioses. *Annu Rev Plant Biol* 64:781–805, 2013).

117. **Venn AA, Tambutté E, Holcomb M, Allemand D, Tambutté S**. Live Tissue Imaging Shows Reef Corals Elevate pH under Their Calcifying Tissue Relative to Seawater. *PLoS ONE* 6: e20013–9, 2011.

118. **Venn AA**, **Tambutté E**, **Lotto S**, **Zoccola D**, **Allemand D**, **Tambutté S**. Imaging intracellular pH in a reef coral and symbiotic anemone. *Proc Natl Acad Sci U S A* 106: 16574–9, 2009.

119. **Veron JEN**. Corals of Australia and the Indo-Pacific. 2nd ed. University of Hawaii Press.

120. **Voet D, Voet J, Pratt C**. *Fundamentals of biochemistry: life at the molecular level* (3rd ed.). Hoboken, NJ. Wiley Publishing, 2008.

121. **Wainwright SA**. Studies of the mineral phase of coral skeleton. *Experimental Cell Research* 34: 213–230, 1964.

122. **Wang JT, Douglas AE**. Essential amino acid synthesis and nitro- gen recycling in an alga-invertebrate symbiosis. *Mar. Biol.* 135:219–222, 1999.

123. **Wang J**, **Douglas AE**. Nitrogen recycling or nitrogen conservation in an alga-invertebrate symbiosis? *J Exp Biol* 201: 2445–2453, 1998.

124. **Weiner ID**, **Verlander JW**. Ammonia Transporters and Their Role in Acid-Base Balance. *Physiol Rev* 97: 465–494, 2017.

125. **Weihrauch D**, **Joseph G**, **Allen P**. Ammonia excretion in aquatic invertebrates: new insights and questions. *J Exp Biol* 221: jeb169219, 2018.

126. **Weihrauch D**, **Wilkie MP**, **Walsh PJ**. Ammonia and urea transporters in gills of fish and aquatic crustaceans. *J Exp Biol* 212: 1716–1730, 2009.

127. **Weihrauch D**, **Ziegler A**, **Siebers D**, **Towle DW**. Active ammonia excretion across the gills of the green shore crab *Carcinus maenas*: participation of Na(+)/K(+)-ATPase, V-type H(+)-ATPase and functional microtubules. *J Exp Biol* 205: 2765–2775, 2002.

128. **Weis VM**, **Allemand D**. What determines coral health? *Science* 324: 1153–1155, 2009.

129. **Weis VM**, **Davy SK**, **Hoegh-Guldberg O**, **Rodriguez-Lanetty M**, **Pringle JR**. Cell biology in model systems as the key to understanding corals. *Trends Ecol Evol* 23: 369–376, 2008.

130. **Wingfield PT**. Protein precipitation using ammonium sulfate. *Curr Protoc Protein Sci* 84: A.3F.1-A.3F.9, 2016.

131. **Wilkie MP**. Ammonia excretion and urea handling by fish gills: Present understanding and future research challenges. In: *Journal of Experimental Zoology*. 2002, p. 284–301.

132. **Wright PA**, **Wood CM**. A new paradigm for ammonia excretion in aquatic animals: role of Rhesus (Rh) glycoproteins. *J Exp Biol* 212: 2303–2312, 2009.

133. **Zoccola D**, **Ganot P**, **Bertucci A**, **Caminiti-Segonds N**, **Techer N**, **Voolstra CR**, **Aranda M**, **Tambutté E**, **Allemand D**, **Casey JR**, **Tambutté S**. Bicarbonate

transporters in corals point towards a key step in the evolution of cnidarian calcification. *Sci Rep* 5: 9983, 2015.

134. **Zoccola, D., Tambutté, E., Sénégas-Balas, F., Michelis, J.-F., Failla, J.-P., Jaubert, J. and Allemand, D**. Cloning of a calcium channel a1 subunit from the reef- building coral, *Stylophora pistillata*. *Gene* 227: 157–167, 1999.